VATNAJÖKULL:
Mass balance, meltwater drainage and surface velocity of the glacial year 2011_12

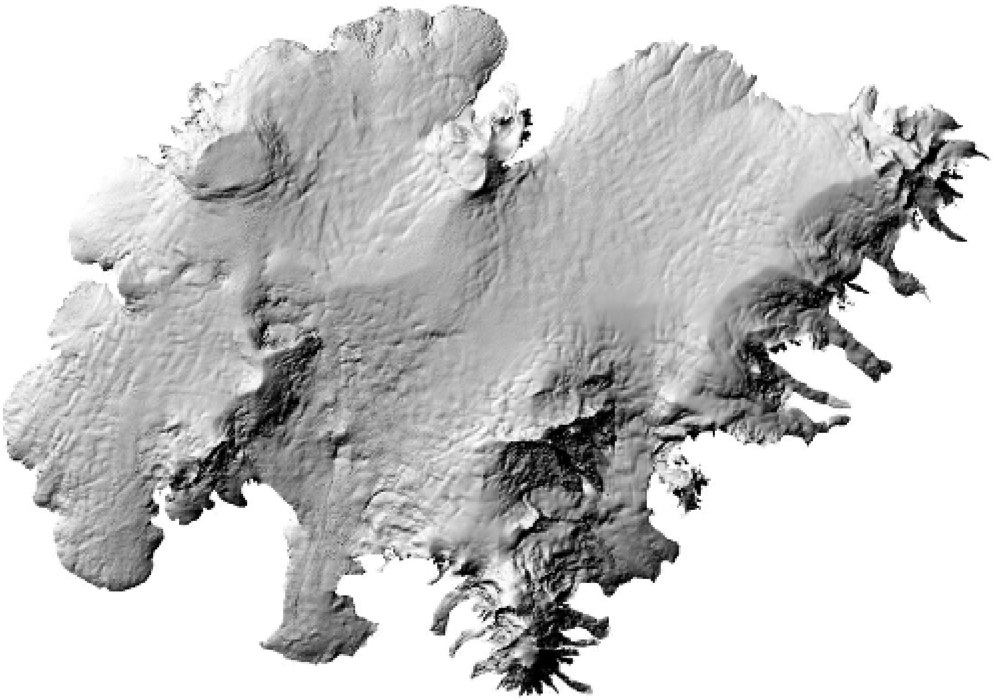

Institute of Earth Sciences
University of Iceland
and
National Power Company

Finnur Pálsson
Helgi Björnsson
Hannes H. Haraldsson
Andri Gunnarsson

RH-25-2013

Contents:

Figures:

Tables:

Appendixes:

1. INTRODUCTION

In 1992 (glacial year 1991_1992) a program of mass balance measurements was started for Vatnajökull by the Science Institute University of Iceland (now Institute of Earth Sciences, IES) in collaboration with the National Power Company (NPC). For the first year the program was limited to the western part of the glacier, but then expanded to include the northern outlets as well. In 1996 this study was further expanded to include southern outlets, with support from The European Union (Framework IV - Environment and Climate, TEMBA project 1996-1997). This program was extended 1998–2000 with further support from EU (Framework IV - Environment and Climate, ICEMASS project, 1998-2000). In 2000-2002 NPC and IES continued the program. In 2003-2005 IES participated in a multinational research project, which was financially supported by The European Union (EVK2-CT-2002-00152 SPICE). IES was responsible for obtaining data sets for calibration of models of the mass balance and dynamics of Vatnajökull. This work was also supported by The National Power Company of Iceland and The National Road Authority, and is a continuation of the TEMBA-project of 1996-97 and ICEMASS project 1998-2001.

In 2011-12 IES and NPC continued a similar program. Mass balance measurements on the southeast outlets Breiðamerkurjökull and Hoffellsjökull is financially supported by the National Road Authority.

The aim of the collaborative work of NPC and IES is to improve our understanding of the mass balance and melt water runoff from glaciers. This work in combination with energy balance measurements by NPC and IES on Vatnajökull will be used for calibration of models of the energy and mass balance of Vatnajökull.

This report describes the field measurements and the initial results, the mass balance and melt water runoff for the glacial year 2011_12.

2. DIARY

March 13-14: GPS survey of sites on Tungnaárjökull.
April 20: winter mass balance measurements, maintenance of AWS on Breiðamerkurjökull.
May 4 - 11: measurements of the winter balance
June 1 - 6: measurements of the winter balance.
July 7: mass balance wires on Breiðamerkurjökull measured.
August 29-30: mass balance measurements, maintenance of AWS on Breiðamerkurjökull
October 8 - 14: summer balance measurements.

In all expeditions and short visits to the glacier the locations of mass balance stakes were measured with Kinematic GPS (or fast static GPS and a few with DGPS) for surface velocity calculation.

The following members of staff of the Institute of Earth Sciences, University of Iceland, carried out the fieldwork on Vatnajökull: Finnur Pálsson, Þorsteinn Jónsson and Sveinbjörn Steinþórsson. Also Hannes H. Haraldsson and Andri Gunnarsson (National Power Company), and Hlynur Skagfjörð Pálsson (Reykjavík Rescue Team). Members of the Iceland Glaciological Society assisted in the June fieldwork.

3. MASS BALANCE MEASUREMENTS

The purpose of the mass balance measurements is to describe the temporal and spatial distribution of the components of the mass balance. The mean annual values of the components and their variation from year to year are analyzed and related to meteoro-logical conditions and climatic variability. The results will be used in studies of changes in the glacier volume, estimates of meltwater contribution to glacial rivers, mass balance modeling, evaluation of altitudinal and regional variations of mass balance in response to climatic variations, and to assess the hydrometeorological and dynamic response of the ice cap to climate change.

The mass balance was determined by a stratigraphic method, measuring changes in thickness and density relative to the summer surface. The winter balance was estimated by drilling ice cores through the winter layer in the spring. Ablation was monitored from markers; snow stakes were put up on the glacier and wires were drilled down in the ablation area. The summer balance was measured in the autumn.

3.1 Methods

Measurements of the surface mass balance on a large ice cap like Vatnajökull are impractical in terms of cost with conventional techniques and sampling density that are typically used on small glaciers. The spatial variability of the mass balance may, however, be predictable on the flat large outlets of such an ice cap given data on several profiles extending over the elevation range of the glacier. The precipitation generally increases with elevation and decreases with the distance from the coast, but both the distribution of snowfall and redistribution of snow by drift depend on the prevailing wind direction during the winter. The summer melting depends mainly on the altitude and the albedo of the glacier surface. Therefore, we have used observations along a limited number of flowlines, which span the elevation range of the outlets to assess aerial estimates of surface mass balance. Each profile describes the variation with elevation, but together they also describe the lateral variation of the mass balance. Recently, modern over-snow vehicles and helicopters have allowed fast traverses to ensure successful fieldwork in spite of frequently poor weather conditions. The error for individual point measurement is estimate ~30 cm_{we} for both summer and winter balance. The error for the area integral of mass balance is however considered smaller, since the error for individual survey sites is independent.

The winter mass balance (b_w) is defined as the mass of snow accumulated during the winter months, the summer balance (b_s) is the mass balance during the summer, and the net balance (b_n) is defined as their sum. The specific mass balance is expressed in terms of the equivalent thickness of water. All mass balance components apply to a time interval between given measurement dates, which are not fixed from one year to another. The dates in the autumn are separated by approximately one calendar year, which roughly coincides with the glaciological year defined as October 1st to September 30th. Snow cores are drilled in April-May through the winter layer and profiles of the density are measured. The summer balance is derived in the autumn from measurements of the changes in the snow core density during the summer in the accumulation area and from readings at stakes and wires drilled into the ice in the ablation areas.

Digital maps are created for winter, summer and net balance for the whole ice cap based on site measurements. The mass balance is calculated over both the ice and water drainage basins. The summer balance over the water basin is an estimate of meltwater contribution to rivers and groundwater storage. This estimate, however, does not include precipitation that falls as rain on the glacier or snow, which falls and melts during the summer. The meltwater contribution is compared with river runoff at stream flow gauges closest to the glacier. For this comparison, we define the glaciological year from the start of October to the end of September and the period draining meltwater from the glacier during the summer from June through September. It would be misleading to include May in the summer period because runoff from the glacier melt in May is delayed due to refreezing during elimination of the cold wave.

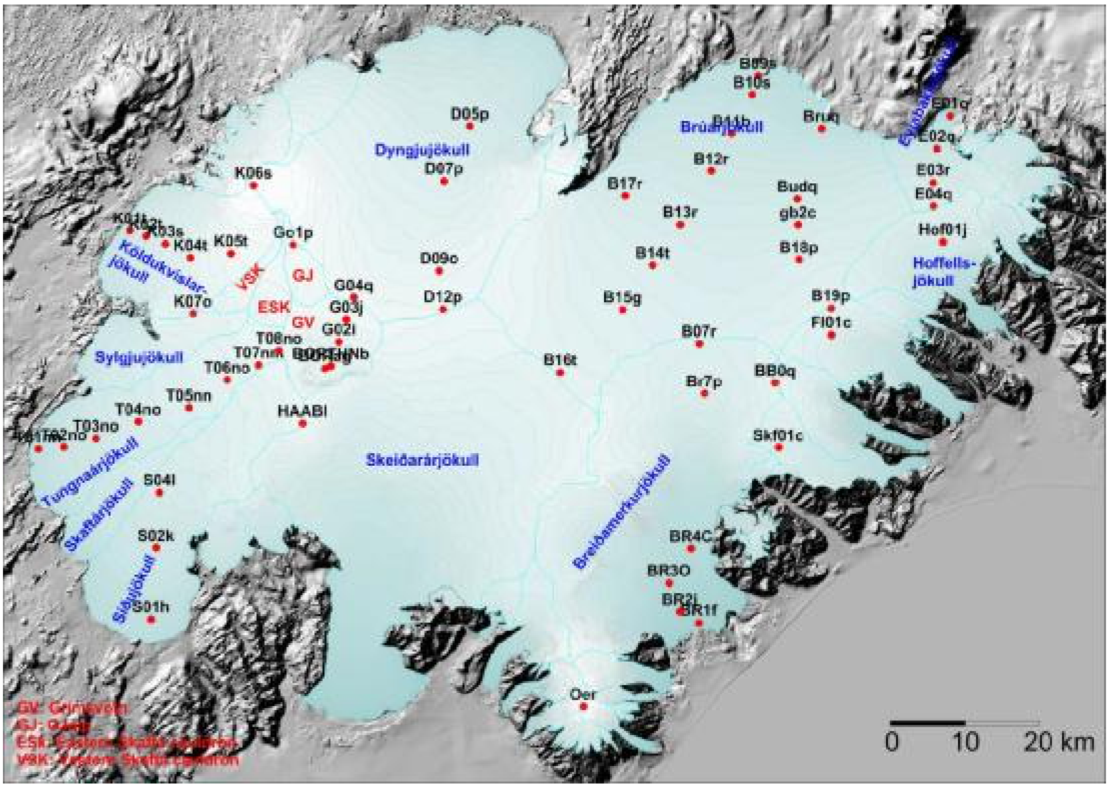

Figure 1. Outlets of Vatnajökull and location of mass balance measurement sites 2011_12.

3. 2 Results of mass balance measurements.

Mass balance measurements were done at 57 sites in spring 2012 (Fig. 1). The specific mass balance at individual sites is shown in Fig. 2. Most sites are on central flow lines at individual outlets. The specific mass balance along flow lines is given in Fig. 3 as a function of elevation for each glacier outlet: Síðujökull, Tungnaárjökull, Dyngjujökull, Köldukvíslarjökull, Brúarjökull (west and east), Eyjabakkajökull, Hoffellsjökull and Breiðamerkurjökull.

Digital maps for winter, summer and net balance are shown in Figure 4. Although no balance measurements are available for Skeiðarárjökull, the balance has been estimated by interpolating the balance values from the neighboring outlets, based on our experience from previous years. The mass balance of individual large outlets is discussed in the following

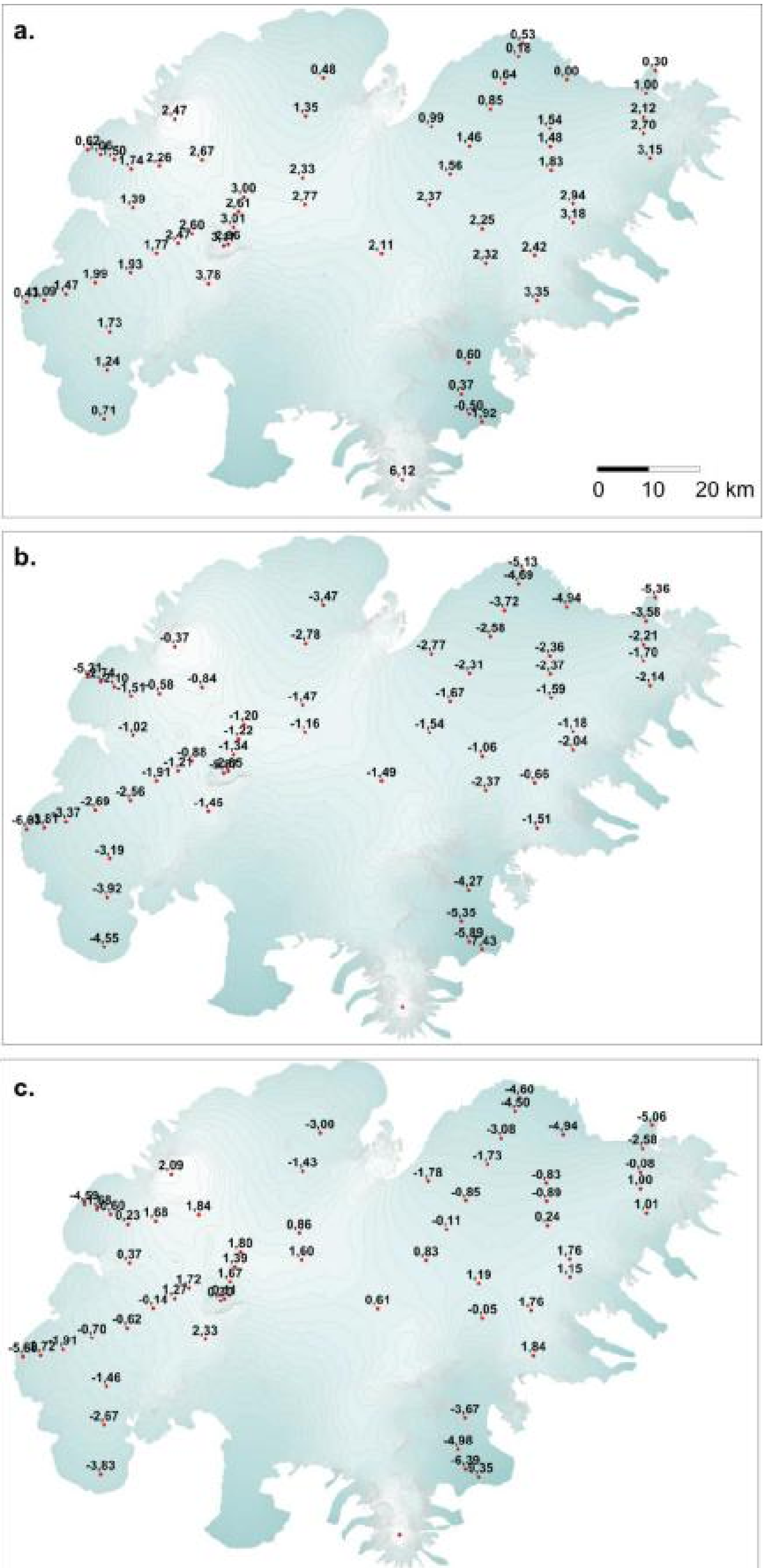

Figure 2. Maps showing point values of specific mass balance in m water equivalent (m_{we}), 2011_12. a. winter, b. summer, c. net balance.

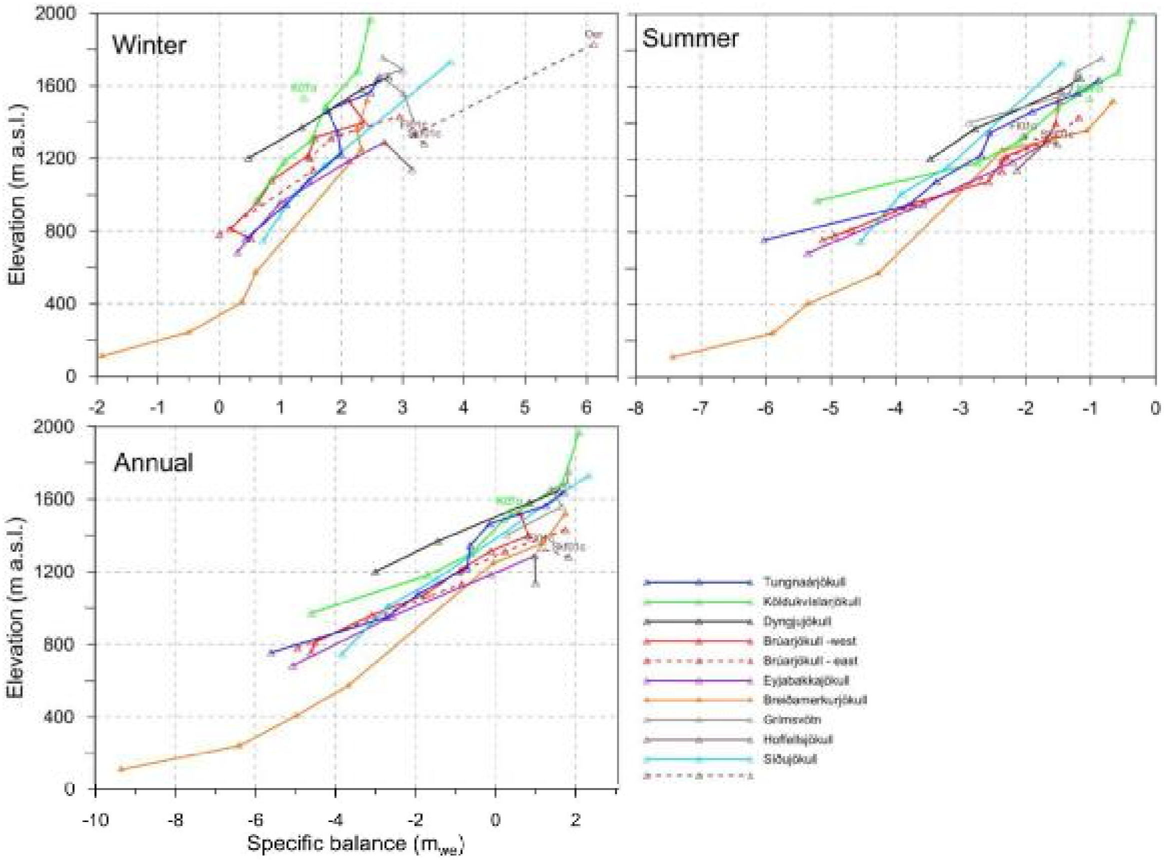

Figure 3a. Specific mass balance (m_{we}), along all mass balance profiles 2011_12.

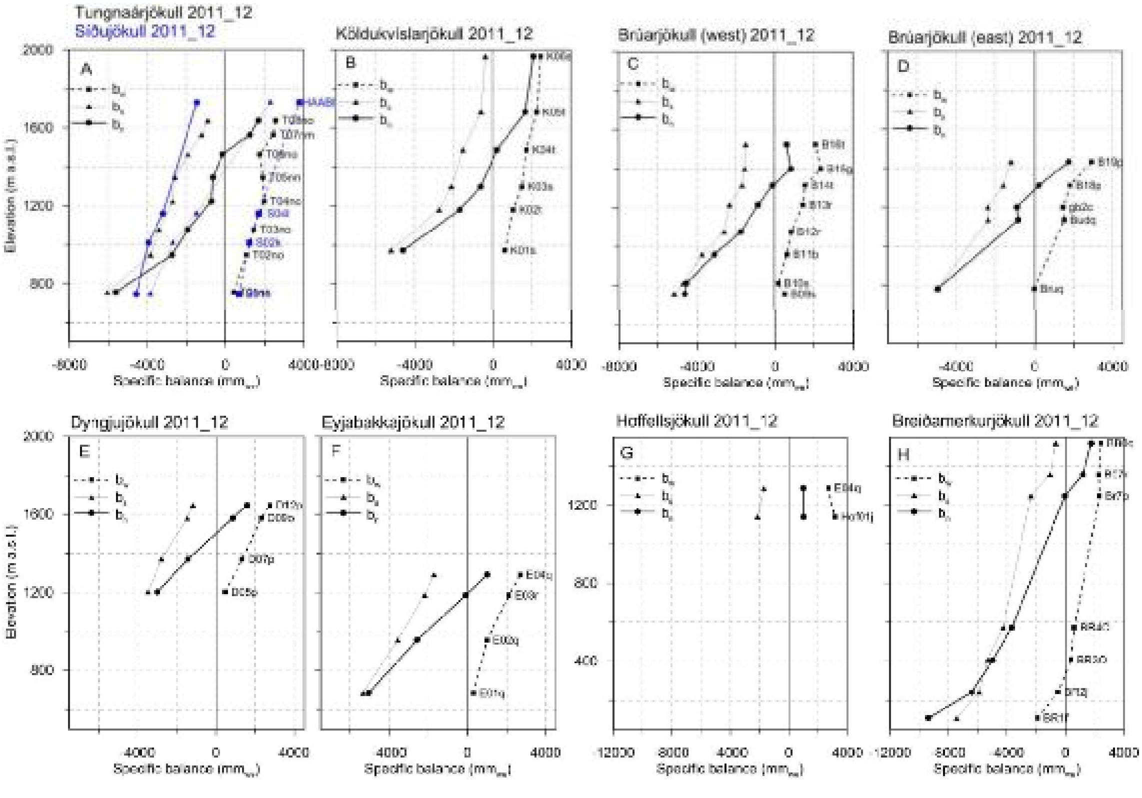

Figure 3b. Specific mass balance (mm_{we}) 2011_12 as a function of elevation on central flow lines on Vatnajökull outlets.

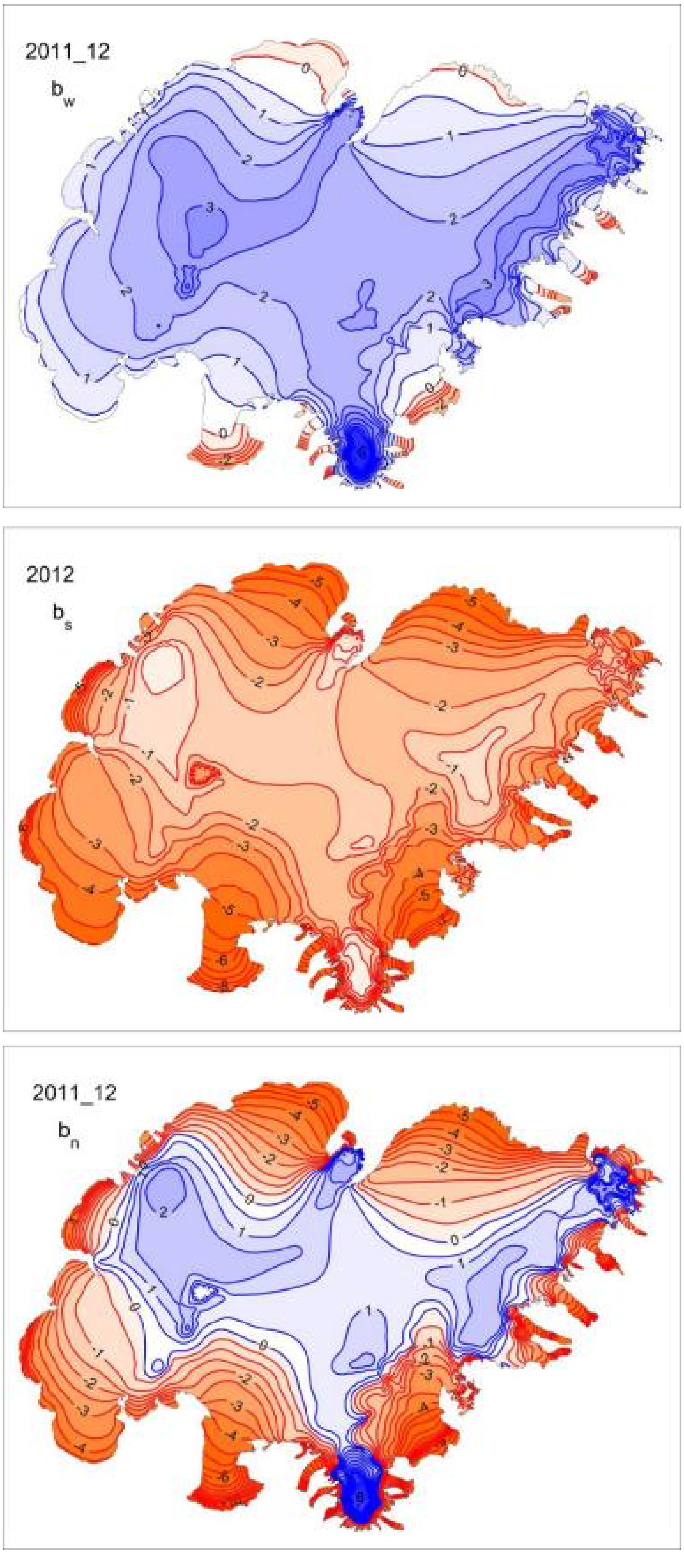

Figure 4. Specific mass balance (m_{we}) maps of Vatnajökull 2011_12. Top: winter, Centre: summer, Bottom: net balance.

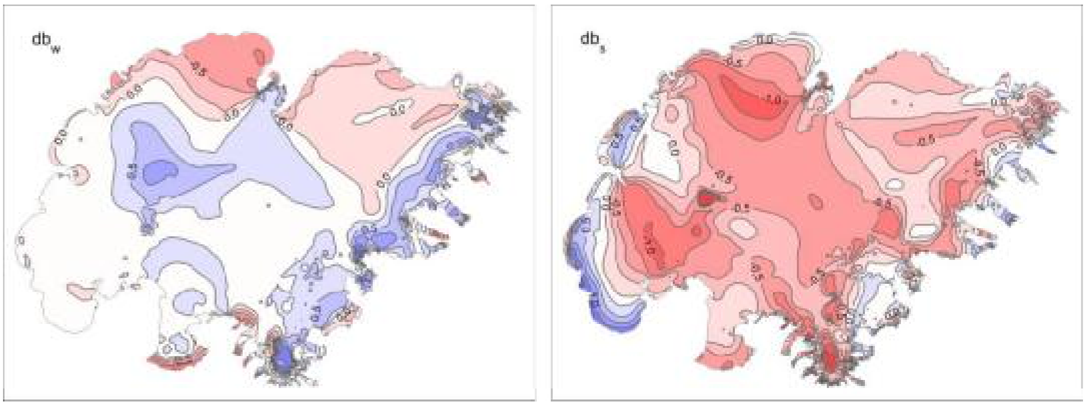

Figure 5. The left frame shows the difference between winter balance in 2011_12 and the average winter balance 1995_96 to 2010_11. (Positive (blue) is higher than average). The left frame shows the difference between summer balance in 2012 and the average summer balance 1996 to 2011. (Negative (red) is higher than average ablation).

subsections. A DEM of Vatnajökull mostly based on SPOT5 HRS images (stereo images from the SPOT5 satellite) in 2010, and partly from LiDAR survey 2010, is used for surface area distribution and delineation of ice divides for individual outlets and catchments.

In the first months of winter precipitation was unusually high in southeast Iceland. The latter half was dominated by unusually high precipitation in west and south Iceland. This is evident in the lower than average (fig. 5) winter snow on the northern outlets, especially on Dyngjujökull (see also Appendix F, MODIS image series for the winter.

The summer 2012 was exceptionally sunny, especially in the southwest. June was exceptionally dry; warm in western Iceland but cold in the east. July was similar, warm, sunny and dry in the southwest but less so in the east, same applies to August. (Information about weather is from the web site of the Iceland met office written by Trausti Jónsson). Inspection of the MODIS monthly overview of the summer months in Appendix F show that days with clear skies over Vatnajökull were 5 in the latter half of May, ~11 in June, 1~12 in July, the week and last few days of August. September was stormy with occasional snowfall in cold northern winds.

The relatively long periods of clear skies, in the months of highest solar angle, combined with dirt blown over the glacier in the dry periods in late May and June, enhanced melting in the upper regions of the glacier (see MODIS images for late May and June in appendix F, prevailing northern winds blow dust from the dry snow free areas north of the glacier). In the upper region of western Vatnajökull tephra blown over the glacier from the Grímsvötn area enhanced ablation. The thin winter snow cover of the ablation zones of the northern outlets also result in enhanced ablation there; the snow cover melts away quickly revealing the bare ice with high content of dark tephra particles that effectively lower the albedo and increase absorption of short wave radiation. All this resulted in (see fig. 5) exceptionally high ablation in the accumulation areas, and the ablation zones of the northern outlets.

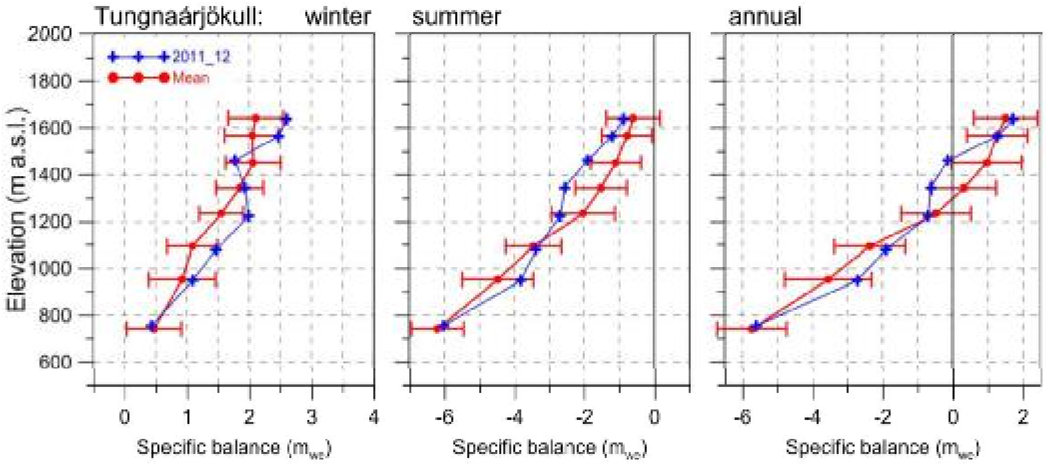

Figure 6. Mass balance at a central flow line of Tungnaárjökull 2011_12, and average mass balance 1991_92 to 2010_11.

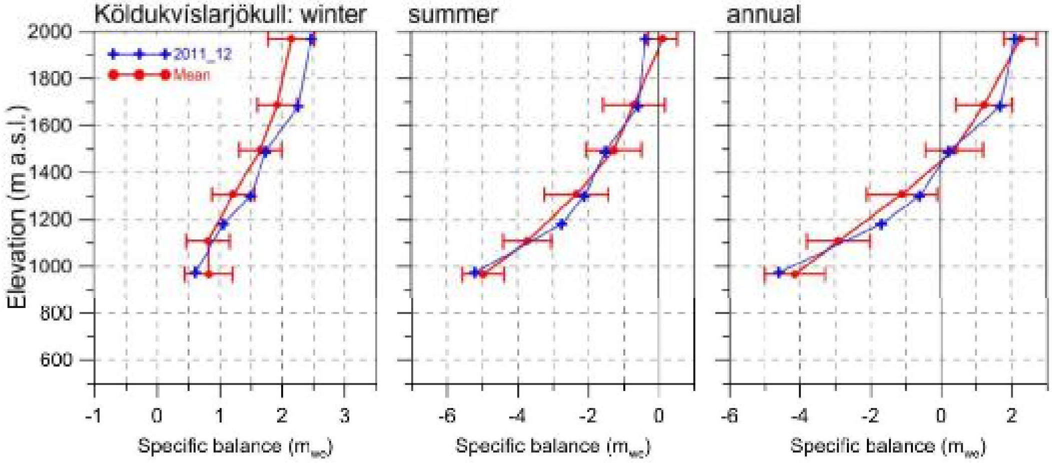

Figure 7. Mass balance at a central flow line of Köldukvíslarjökull 2011_12, and average mass balance 1991_92 to 2010_11.

3.2.1 Tungnaárjökull.

Area = 345 km^2
B_w= 0.49 km^3 ; b_w = 1.63 m
B_s = -1.01 km^3 ; b_s = -2.93 m
B_n = -0.45 km^3 ; b_n = -1.30 m
ELA = 1420 m (at profile)
AAR = 21 %

(The terms are defined at the foot of this page)

Variation of mass balance along a central flow line on Tungnaárjökull is shown in Fig. 6. The winter balance was higher than average at most sites of the survey sites. The seeming strange low at 1300-1500 m elevation may result that neither precipitation from the northern or the southwest reached there. Winter balance was 11% higher than average. Summer melting was more than average at the upper sites, but less than average in the ablation zone, probably due to the thick winter snow cover and less sunlight. The total ablation was 10% above average during the survey period. The net balance was negative the 18th year in a row; the loss was 0.1 m_{we} more than average during the survey period, (8% more than average).

3.2.2 Köldukvíslarjökull

Area = 301 km^2
B_w = 0.49 km^3 ; b_w = 1.64 m
B_s = -0.58 km^3 ; b_s = -1.93 m
B_n = -0.09 km^3 ; b_n = -0.29 m
ELA = 1433 m (at profile)
AAR = 51 %

B_w,B_s and B_n are water equivalent volumes of winter, summer and net balance, ELA the equilibrium line altitude, and AAR is the accumulation area ratio.

Variation of mass balance along a central flow line on Köldukvíslarjökull is shown in Fig. 7. Accumulation was about one st.var. over the average at the highest survey sites, but close or lower than average at the lowest. The winter balance was about 13% higher than average since 1991_92, and the summer balance 96% of the average. The net balance was negative the 18th year in a row, by 55% of the average during the survey period (0.25 m_{we} less than average).

3.2.3 Dyngjujökull

Area = 1064 km^2
B_w= 1.58 km^3 ; b_w= 1.48 m
B_s = -2.61 km^3 ; b_s = -2.46 m
B_n = 1.03 km^3 ; b_n = -0.98 m
ELA = 1500 m (at profile)
AAR = 47 %

Variation of mass balance along a flow line on Dyngjujökull is shown on Fig. 8. The winter balance in 2010_11 was more than std.var. above average in the uppermost survey sites, but more than std. var. less at 1200 m, and almost nothing was accumulated in the ablation zone (no sites but this is obvious from the MODIS images in appendix F.) In total the winter balance was 10% higher than average.

The summer ablation was close to average at all sites. The net balance was slightly positive. Mass balance is not measured at the lowest elevations, but assumed to be similar (as a function of elevation) to that of Brúarjökull and Köldukvíslarjökull.

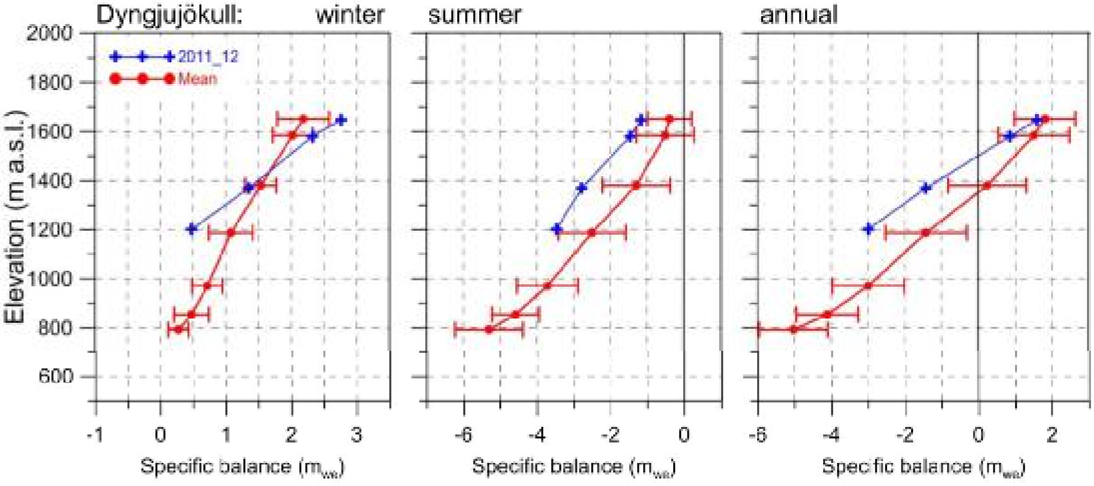

Figure 8. Mass balance at a central flow line on Dyngjujökull 2011_12, and average mass balance 1991_92 to 2010_11 (except 1998_99 – 2003_04 at all but the top elevation).

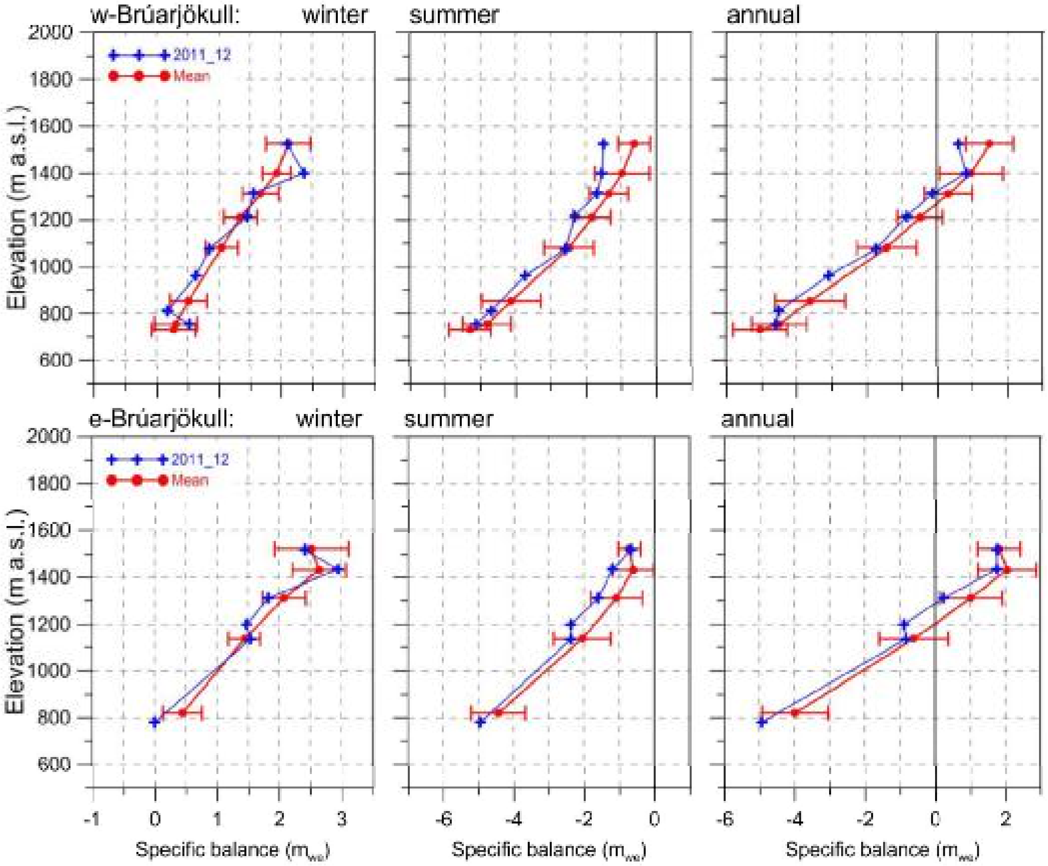

Figure 9. Mass balance at two flow lines on Brúarjökull 2011_12, and average mass balance 1992_93 to 2010_11.

3.2.4 Brúarjökull

Area = 1526 km^2
B_w= 2.35 km^3 ; b_w = 1.54 m
B_s = -3.51 km^3 ; b_s = -2.30 m
B_n = -1.16 km^3 ; b_n = -0.76 m
ELA = 1322 m (western flow line)
ELA = 1295 m (eastern flow line)
AAR = 45 %

Variation of mass balance along two flow lines on Brúarjökull is shown on Fig. 9. At all the lower survey sites accumulation was significantly (almost 1 std. dev.) less than average, but in the large area between ~1300-1500 m the winter snow accumulation was well above average. This resulted in total winter balance slightly higher (1%) than average. The thin snow cover of the ablation zone, dirt blown over the glacier in May and June and relatively clear skies during the ablation season resulted in summer ablation about 20% above the average. Most of this increase is in the accumulation area, the result of lower albedo due to the dirty summer surface. At the highest survey site the summer ablation is close to average, this is due to occasional snow fall during the summer, effectively heightening the average surface albedo. The net mass loss was about twofold the average of the survey period.

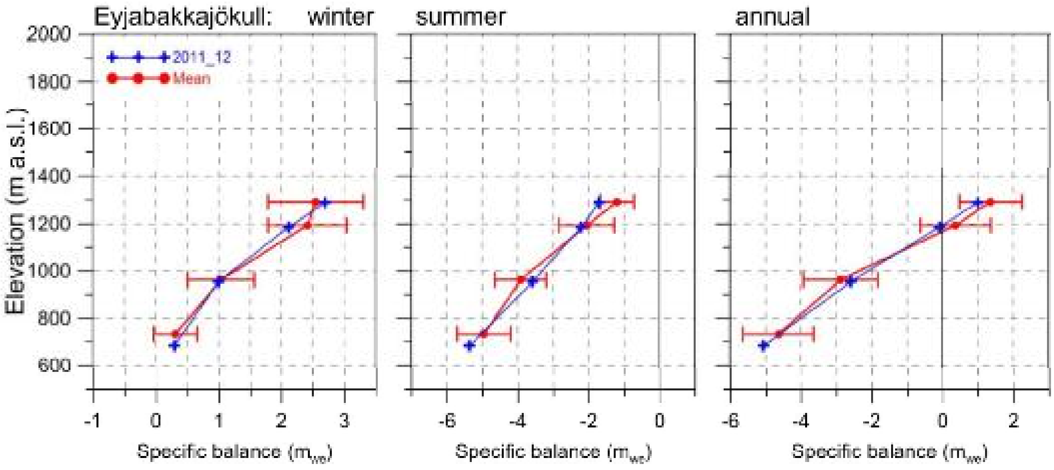

Figure 10. Mass balance at a central flow line of Eyjabakkajökull 2011_12 and average mass balance 1995_96 to 2010_11.

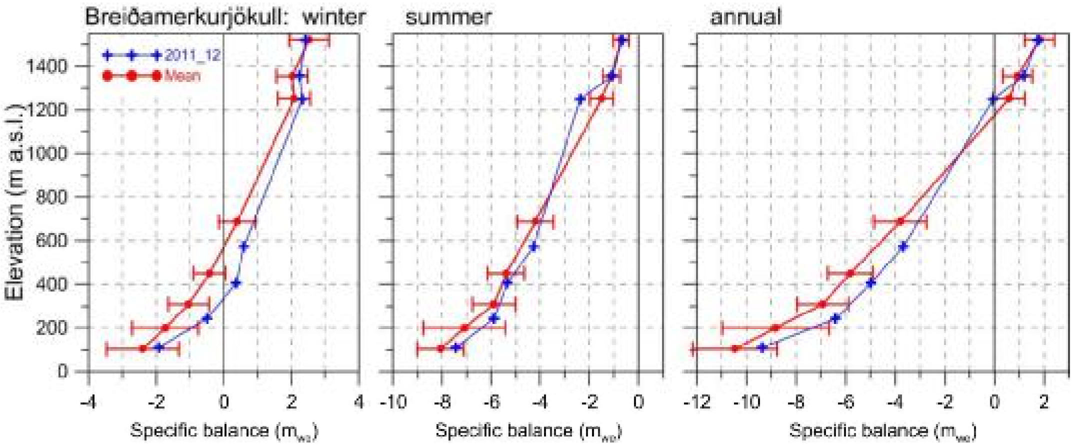

Figure 11. Mass balance at a central flow line of Breiðamerkurjökull 2011_12, and average mass balance 1995_96 to 2010_11.

3.2.5 Eyjabakkajökull

Area = 112 km^2
B_w= 0.20 km^3 ; b_w = 1.80 m
B_s = -0.31 km^3 ; b_s = -2.76 m
B_n = -0.11 km^3 ; b_n = -0.96 m
ELA = 1193 m (at profile)
AAR = 33 %

Variation of mass balance along a central flow line on Eyjabakkajökull is shown on Fig. 10. Winter balance was slightly higher than average in the mid and elevation range, in total the winter balance was 5% higher than average. Summer ablation was close to average except at the highest elevation, dirt enhanced ablation (see. Appenix F). The total ablation was 99% of the average. The annual balance was negative, 90% of the average since 1995_96.

3.2.6 Breiðamerkurjökull

Area = 938 km^2
B_w= 1.60 km^3 ; b_w = 1.70 m
B_s = -2.62 km^3 ; b_s = -2.79 m
B_n = -1.02 km^3 ; b_n= -1.09 m
ELA = 1250 m (at profile)
AAR = 47 %

Variation of mass balance along a

central flow line on Breiðamerkurjökull is shown on Fig. 11. Snow accumulation was close to average in the upper area, but much higher than average (more than std. dev.) in the lower area. The winter ablation at the lowest survey sites was also significantly less than average. The winter was rather cold, and with high precipitation in the south. The winter balance was 30% above average. Ablation was 7% of the average; the warm and sunny summer did not dominate this part of the country. The net balance was negative but only 85% of the average.

3.3 The mass balance record for Vatnajökull.

From the digital maps the total volumes of winter, summer and net balance have been calculated by integration (appendix D, gives balance values as a function of elevation) and are as follows:

$\mathbf{B_w = 13.56\ km^3\ ;\ b_w = 1.70\ m}$
$\mathbf{B_s = -20.43\ km^3\ ;\ b_s = -2.56\ m}$
$\mathbf{B_n = -6.87\ km^3\ ;\ b_n = -0.86\ m}$
AAR = 46%

Most of the winter was wet, with prevailing southerly winds. This lead to higher than average winter balance by 30% (over the observation period 1991_92-2011_12, Fig. 12). The zero mass balance turnover for Vatnajökull (current topography) is close to 13.4 km^3 (1.64 m w. eq.) and the winter balance 2011_12 is about 4% higher. The relatively long periods of clear skies, in the months of highest solar angle, combined with dirt blown over the glacier in the dry periods in late May and June, enhanced melting in the upper regions of the glacier. In the upper region of western Vatnajökull tephra blown over the glacier from the Grímsvötn area enhanced ablation. The thin winter snow cover of the ablation zones of the northern outlets also result in enhanced ablation there; the snow cover melts away quickly revealing the bare ice with high content of dark tephra particles that effectively lower the albedo and increase absorption of short wave radiation. All this resulted exceptionally high ablation in the accumulation areas, and the ablation zones of the northern outlets.

The summer ablation was ~27% higher than average over the survey period, 56% higher than for zero balance turnover. The net balance was negative, the mass loss was 16% more than average (-0.74 m) of the past 17

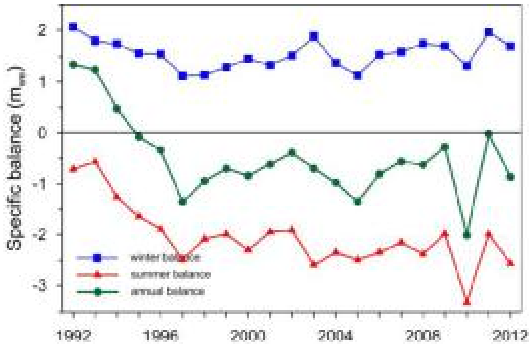

Figure 12. Specific mass balance record for Vatnajökull 1991_92 – 2011_12.

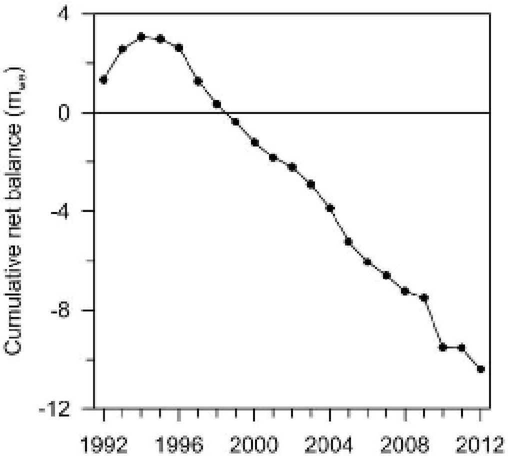

Figure 13. Cumalative specific mass balance of Vatnajökull 1991_92 – 2011_12.

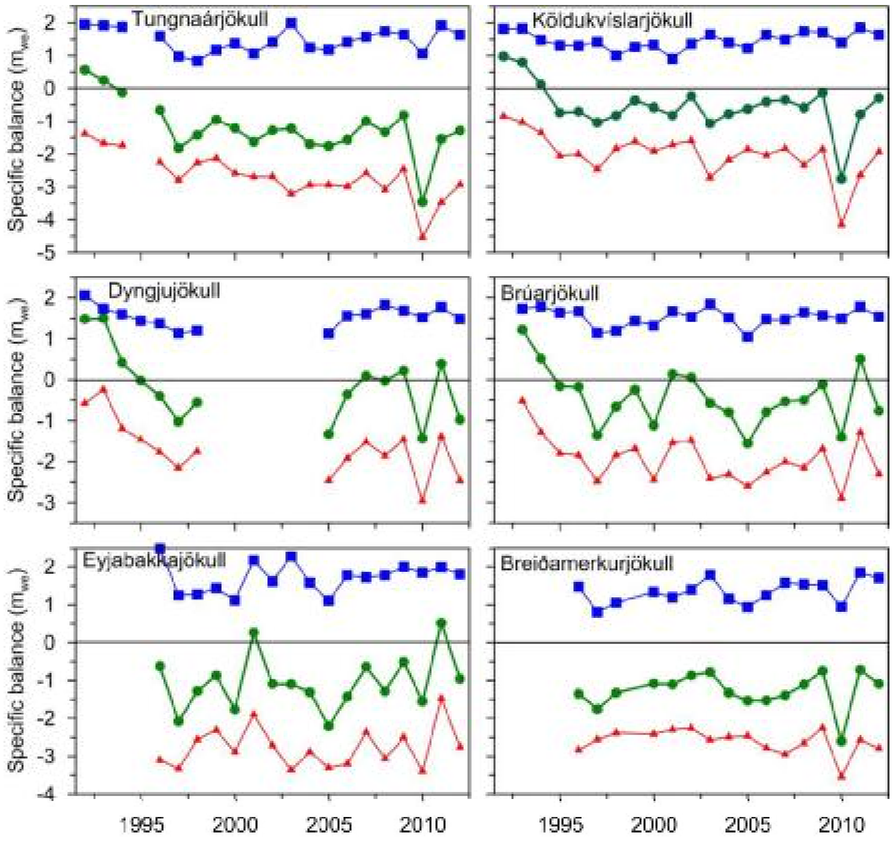

Figure 14. Specific mass balance record for Vatnajökull outlets 1991_92-2011_12.

consecutive years of negative balance.

The glacial year of 2011_12 was the 18th in a row with negative mass balance for Vatnajökull (Fig. 12, Fig. 13), contributing to a total loss of 13.5 m$_{we}$ (ice volume of ~120 km^3) since 1994_95.

The temporal variability of mass balance for different outlets is shown in Fig. 14. The greatest variability of the winter balance is for Eyjabakkajökull, the eastern most of studied outlets. This part of the glacier receives precipitation from all south- and east- and north-easterly wind directions, and thus has high snow accumulation in winters when the paths of the North Atlantic lows is just east of Iceland. This is also the case for the eastern part of Brúarjökull.

Breiðamerkurjökull shows lowest variability. It is a maritime glacier with climate controlled by the stable sea temperature and humid air mass. The longest winter balance records seem to reveal periodic behaviour, with peaks in ~1991_92 and 2002_03 and a low in ~1998. During the period of net mass loss since 1994_95, the

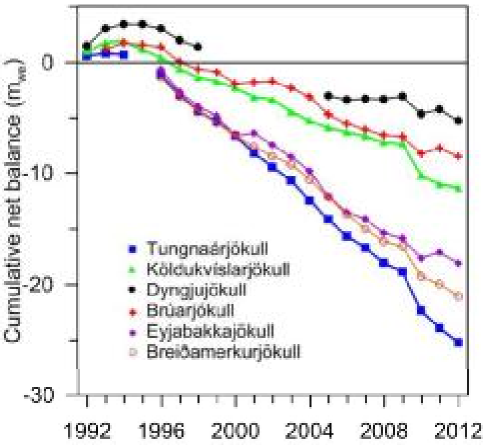

Figure 15. Cumulative specific mass balance for several of Vatnajökull outlets 1991_92 – 2011 12.

northern outlets have had several years of close to zero and positive mass balance. The cumulative net balance curves for the outlets of Vatnajökull in Fig. 15 show that all outlets have been losing mass since 1994_95. The slope for mass loss is about 0.7 ma^{-1} for the northern outlets, but 1.5 ma^{-1} for the south and western outlets.

In Fig. 16 the relation of the annual net balance to the accumulation area ratio (AAR) and equilibrium line altitude (ELA) is shown for different outlets over the survey period. The b_n-AAR gradient is similar for all outlets, about 0.5 m_{we} for 10% change in AAR. The zero-balance AAR varies for different outlets from about 60-65%, similar for all outlets except for the southern outlet Breiðamerkurjökull.

Breiðamerkurjökull is not in dynamic or mass balance equilibrium, the ablation area is too large. A large part of the glacier has carved 200-300 m through the former sediment bed, and the surface elevation has lowered accordingly. Breiða-merkurjökull is now retreating at a high rate.

Similarly the zero-balance ELA varies from about 1000-1100 m for the southern outlets to 1400 m for the NW outlets. The b_n-ELA slope is similar for all outlets -0.7 m_{we} per 100 m.

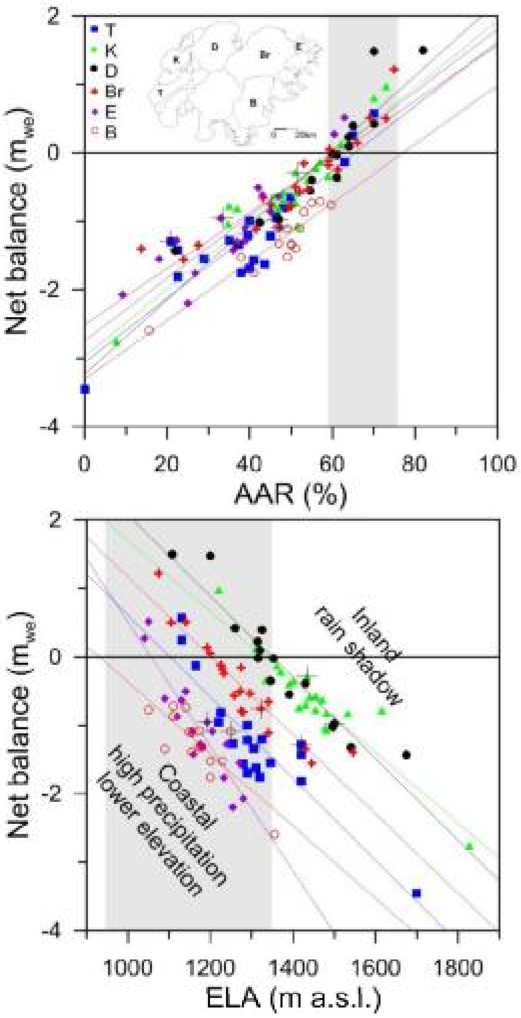

Figure 16. The relation between net annual balance (b_n) and accumulation area ratio (AAR)(upper) and b_n and equilibrium line altitude (ELA), for Vatnajökull outlets during the survey period. (This year's points are marked with a black +).

4. SURFACE VELOCITY MEASUREMENTS

The surface velocity of the glacier was calculated from DGPS (accuracy within 1 m), fast static (accuracy about 1 cm) and kinematic GPS (accuracy about 3 cm) positioning of the ablation stakes. All sites were surveyed in spring and autumn (most kinematic, some DGPS), and many also in June (kinematic), August (fast static) and October (kinematic). At a few sites stakes from previous years were found and resurveyed, making it possible to calculate surface velocity over a year or longer time span. The average summer surface velocity is shown on Figure 19.

The use of more accurate instruments and setup, allows estimation of vertical as well as horizontal velocities. Two 6 metre long 4 inch metal poles where set up in the accumulation zone of the western outlet Tungnaárjökull and one on east Brúarjökul to directly measure the vertical displacement. Small GPS units are also attached to the poles and run continuously. At sites close to the glacier edge very small horizontal movement is measured. This indicates that the glacier snouts are almost stagnant. In the centre areas of some of the outlets especially close to the equilibrium line, there is an increase in velocity during summer compared to winter. The summer velocity is of the order of two-fold the winter velocity. This suggests that basal sliding is increased in the melting season, and is of the same magnitude as the deformation velocity.

From previous velocity measurements, surging of outlets has been predicted. No signs of a starting surge are seen from this year's survey.

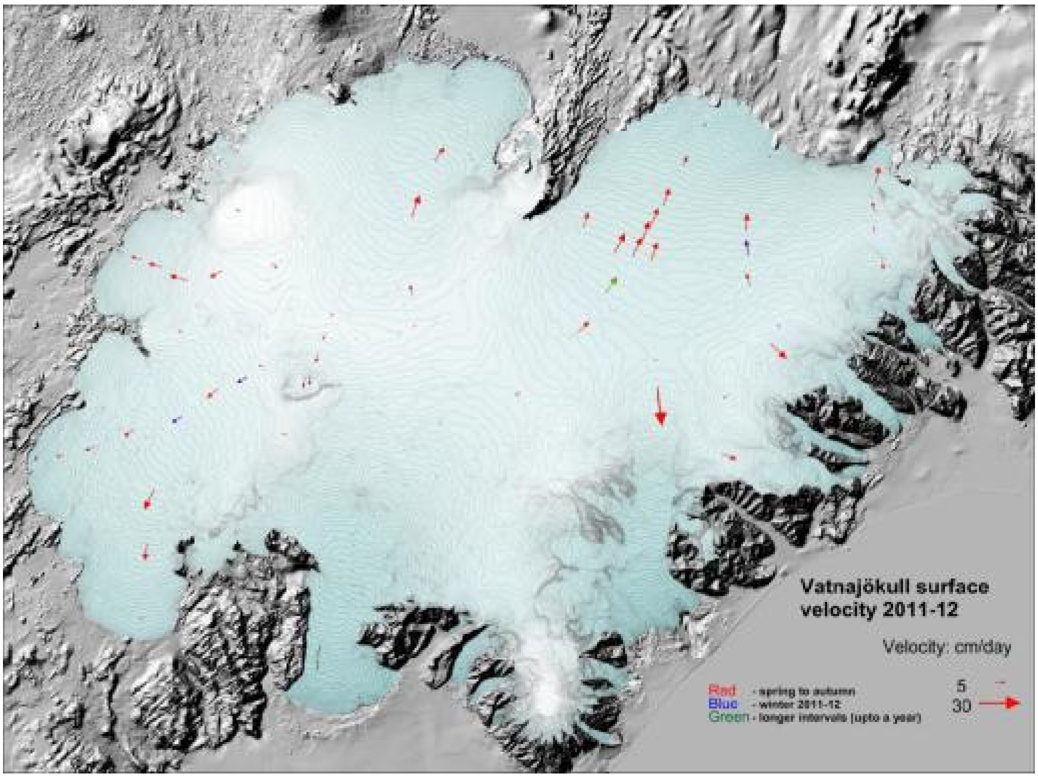

Figure 17. Average surface velocity at survey sites in 2011_12.

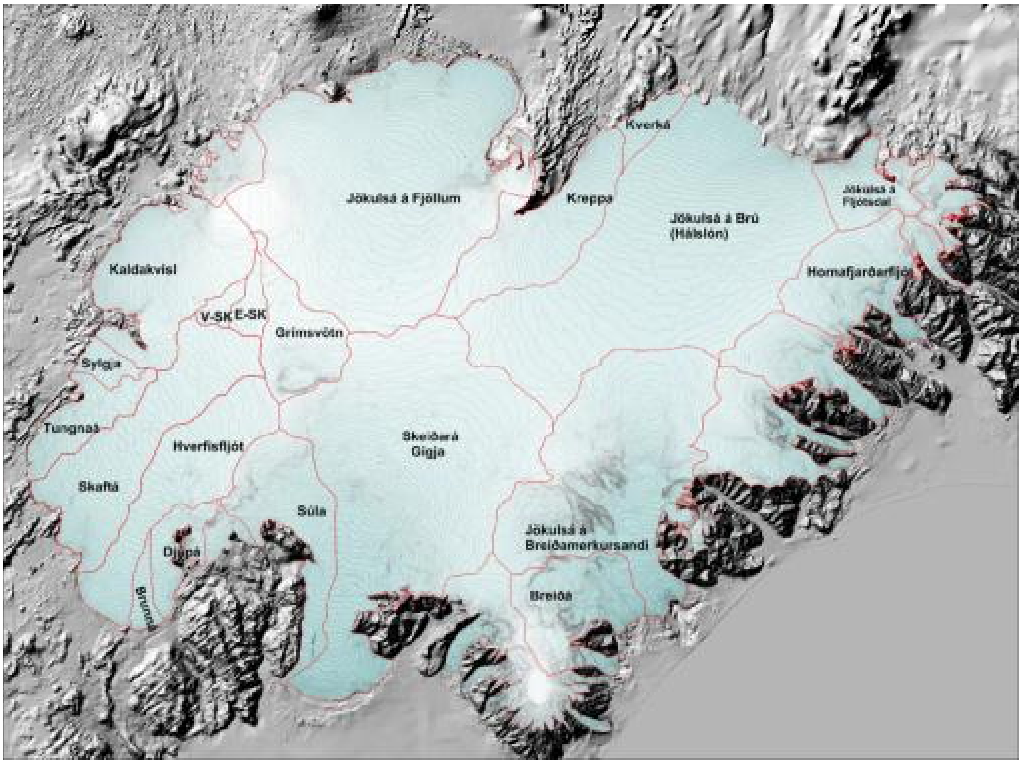

Figure 18. Water divides and drainage basins of selected rivers draining water from Vatnajökull.

5. Melt water runoff.

Water divides and drainage basins for rivers draining water from Vatnajökull have been defined from water pressure potential maps. The potential maps were produced from existing surface (year 2010) and bedrock digital elevation models.

Figure 18 shows the water divides and drainage areas for selected rivers draining melt water from Vatnajökull. The summer balance over the water basin is an estimate of meltwater contribution to rivers and groundwater storage. This estimate, however, does not include precipitation that falls as rain on the glacier, nor snow which falls and melts during the summer. The meltwater contribution can be compared with river runoff at stream flow gauges closest to the glacier. For this comparison, we define the glaciological year from the start of October to the end of September and the period draining meltwater from the glacier during the summer from June through September. It would be misleading to include May in the summer period because runoff from

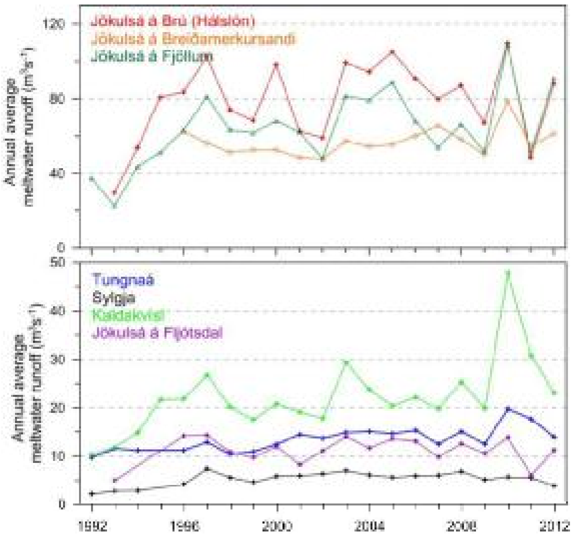

Figure 19. The temporal variation of average annual meltwater runoff to selcted river catchments.

Table I. Melt water drainage to selected rivers in 2011_12.

Water Catchment:	**Area (km^2)**	**ΣQ_s ($10^6 m^3$)**	**Q_s ($m^3 s^{-1}$)**	**Q_a ($m^3 s^{-1}$)**	**q_s ($ls^{-1} km^{-2}$)**
Vatnajökull	7968,0	20438,9	1939,03	648,11	81,34
Tungnaá	121,8	439,9	41,73	13,95	114,52
Sylgja	39,7	122,2	11,59	3,87	97,61
Kaldakvísl	367,9	725,6	68,84	23,01	62,54
Jökulsá á Fjöllum	1188,3	2870	272,28	91,01	76,59
Kreppa	291,2	569,4	54,02	18,06	62,00
Kverka	47,0	208,7	19,80	6,62	140,80
Jökulsá á Brú	1214,8	2768,9	262,68	87,80	72,28
Jökulsá í Fljótsdal	130,6	354,2	33,60	11,23	86,00
Jökulsá í Lóni	101,3	265,9	25,23	8,43	83,23
Hornafjarðarfljót	239,1	593,3	56,29	18,81	78,68
Jökulsá á Breiðamerkursandi	739,5	1932	183,29	61,26	82,84
Breiðá-Fjallsá	234,6	838	79,50	26,57	113,27
Skeiðará-Gígja	1165,2	2983,5	283,04	94,61	81,19
Súla	255,8	904,9	85,85	28,69	112,17
Brunná	35,8	159	15,08	5,04	140,83
Djúpá	83,7	321,8	30,53	10,20	121,91
Hverfisfljót	317,7	895,8	84,98	28,41	89,41
Skaftá	394,9	1127	106,92	35,74	90,50
Grímsvötn	173,3	239,9	22,76	7,61	43,90
Eystri Skaftárketill	39,4	29,2	2,77	0,93	23,50
Vestari Skaftárketill	25,1	16,7	1,58	0,53	21,10
Hólmsá	164,9	464,2	44,04	14,72	89,26
Heinabergsvötn	229,6	645,9	61,28	20,48	89,20
Skjálfandafljót	71,9	123,2	11,69	3,91	54,33

ΣQ_s: total summer melt water; Q_s : average runoff (averaged over summer, 4 months, June – September)
Q_a : average runoff (averaged over a whole year); q_s : average runoff per km^2 (averaged over a whole year)

the glacier melt in May is delayed due to refreezing during elimination of the cold wave and because of the contribution of the spring melt from the highlands to the runoff. Some melting also occurs during winter, especially in the low snouts of the southern outlets.

Average melt water runoff to different rivers is given in Table I, and temporal variation of the average meltwater runoff in Fig. 21. The average specific runoff (q_s) differs from basin to basin from 21 to 140 $ls^{-1}km^{-2}$. This is mainly due to different elevation distributions, for example, the water drainage basins for Tungnaá and Kverká are within the ablation area, while that of Grímsvötn and Skaftárkatlar are high in the accumulation zone.

6. Conclusions

In the first months of winter precipitation was unusually high in southeast Iceland. The latter half of winter was dominated by unusually high precipitation in west and south Iceland.

The summer 2012 was exceptionally sunny, especially in the southwest. June was remarkably dry; warm in western Iceland but cold in the east. July was similar, warm, sunny and dry in the southwest but less so in the east, the same applies to August-September which were stormy with occasional snowfall in cold northern winds.

The relatively long periods of clear skies, in the months of highest solar angle, combined with dirt blown over the glacier in the dry periods in late May and June, enhanced melting in the upper regions of the glacier. In the upper region of western Vatnajökull tephra blown over the glacier from the Grímsvötn area enhanced ablation. The thin winter snow cover of the ablation zones of the northern outlets also result in enhanced ablation there; the snow cover melts away quickly revealing the bare ice with high content of dark tephra particles that effectively lower the albedo and increase absorption of short wave radiation. All this resulted in exceptionally high ablation in the accumulation areas, and the ablation zones of the northern outlets.

The winter balance (13.56 km^3) was higher than average by 30% (over the observation period 1991_92-2011_12). The summer ablation (-20.43 km^3) was ~27% higher than average over the survey period. The net balance was negative (-2.56 km^3), the mass loss was 16% more than average (-0.74 m) of the past 17 consecutive years of negative balance. The accumulation area ratio was 46% for the total glacier. The glacial year of 2011_12 was the 18th in a row with negative mass balance for Vatnajökull (since 1994_95) contributing to a total loss of 13.5 m_{we}, 0.75 $m_{we}a^{-1}$ or an average surface lowering of 0.83 ma^{-1}. This is equivalent to a total ice volume of ~120 km^3, or ~4% off the total ice mass of Vatnajökull.

Summary:

B_w of 13.56 km^3, B_s : -20.43 km^3 and B_n : -2.56 km^3 , AAR = 46%

Specific values:

b_w= 1.70 m, b_s= -2.56, b_n= -0.86 m

Appendix A: Mass balance at measurement sites 2011_12.

b_w: specific winter balance, **b_s**: specific summer balance, **b_n**: specific net balance,
l_a: new snow in autumn (at time of winter survey, autumn date), all in water equivalent.

Site	Position				Elevation	Date	Date	b_w	b_s	b_n	la
	Latitude		Longitude		(m a.s.l.)	in spring	in autumn	(mm)	(mm)	(mm)	(mm)
B09s	64	45,043	16	5,473	757,4	120510	121010	530	-5129	-4599	140
B10s	64	43,685	16	6,701	811,7	120510	121010	181	-4686	-4505	140
B11b	64	40,944	16	10,489	962,0	120510	121009	638	-3716	-3078	263
B12r	64	38,273	16	14,128	1077,1	120510	121009	850	-2578	-1728	315
B13r	64	34,522	16	19,761	1214,6	120509	121009	1455	-2310	-855	298
B14t	64	31,640	16	24,696	1314,3	120510	121010	1560	-1670	-110	224
B15g	64	28,485	16	30,007	1399,1	120510	121010	2373	-1539	834	228
B16t	64	23,569	16	42,066	1523,9	120507	121014	2109	-1494	615	385
B17r	64	36,737	16	28,802	1212,4	120509	121009	987	-2769	-1782	270
BR1f	64	5,520	16	19,485	111,2	120420	120930	-1920	-7434	-9354	
BR2j	64	6,404	16	22,548	241,9	120420	120930	-500	-5895	-6395	
BR3O	64	8,531	16	24,137	406,2	120420	120930	370	-5347	-4977	
BR4C	64	11,757	16	22,124	572,7	120420	120930	600	-4272	-3672	
Br7p	64	22,143	16	16,951	1248,1	120507	121008	2320	-2366	-46	291
B07r	64	25,798	16	17,441	1357,4	120507	121008	2250	-1062	1188	193
BB0q	64	22,717	16	5,051	1519,4	120508	121008	2417	-659	1758	301
Bruq	64	40,998	15	55,222	781,3	120509	121008	0	-4941	-4941	130
Budq	64	35,989	15	59,898	1135,0	120509	121008	1536	-2364	-828	315
gb2c	64	34,093	16	0,021	1200,1	120508	121009	1475	-2366	-891	333
B18p	64	31,58	16	0,11	1311,4	120508	121008	1830	-1590	240	385
B19p	64	27,933	15	55,170	1432,7	120508	121008	2945	-1184	1761	434
D05p	64	42,218	16	54,628	1201,4	120507	121013	476	-3473	-2997	147
D07p	64	38,286	16	59,241	1369,2	120507	121013	1350	-2780	-1430	322
D09o	64	31,801	17	0,551	1580,6	120507	121013	2329	-1465	864	
D12p	64	28,985	17	0,138	1647,7	120507	121010	2765	-1162	1603	287
E01q	64	41,516	15	33,409	683,5	120509	121008	298	-5356	-5058	35
E02q	64	39,138	15	35,970	955,0	120509	121008	995	-3578	-2583	245
E03r	64	36,668	15	36,910	1186,0	120509	121008	2120	-2205	-85	347
E04q	64	34,950	15	37,096	1288,9	120509	121008	2700	-1704	996	350
Hof01j	64	32,327	15	35,838	1140,3	120508	121009	3151	-2143	1008	53
K01s	64	35,350	17	52,772	973,0	120505	121012	619	-5209	-4590	35
K02t	64	34,817	17	49,688	1180,6	120505	121012	1060	-2743	-1683	81
K03s	64	34,245	17	46,377	1299,4	120505	121012	1500	-2103	-603	186
K04t	64	33,211	17	42,247	1488,3	120505	121012	1740	-1512	228	182
K05t	64	33,451	17	35,430	1680,9	120505	121011	2262	-582	1680	378
K06s	64	38,3509	17	31,362	1968,4	120603	121011	2468	-374	2094	585
K07o	64	29,1218	17	42,025	1535,1	120511	121011	1385	-1019	366	214
S01h	64	7,00403	17	49,99	747,5	120505	121012	714	-4548	-3834	18
S02k	64	12,156	17	48,978	1011,3	120505	121012	1244	-3917	-2673	154
S04l	64	16,200	17	48,227	1161,0	120505	121012	1725	-3188	-1463	210

T01nn	64	19,4844	18	8,2293	756,3	120504	121012	430	-6028	-5598	18
T02no	64	19,604	18	3,948	948,6	120504	121012	1094	-3812	-2718	126
T03no	64	20,204	17	58,588	1079,0	120504	121012	1466	-3374	-1908	280
T04no	64	21,339	17	51,499	1223,6	120504	121012	1990	-2688	-698	189
T05nn	64	22,298	17	42,972	1344,7	120504	121012	1934	-2557	-623	350
T06no	64	24,287	17	36,531	1464,4	120504	121012	1769	-1906	-137	571
T07nm	64	25,301	17	31,193	1564,0	120505	121012	2473	-1205	1268	298
T08no	64	26,307	17	27,778	1637,2	120505	121012	2597	-877	1720	396
BORTHNb	64	25,10	17	19,15	1402,4	120603	121013	2958	-2850	108	595
BORag	64	24,937	17	20,147	1402,7	120603	121013	3174	-2874	300	350
G02i	64	26,858	17	17,720	1561,0	120603	121011	3010	-1336	1674	291
G03j	64	28,449	17	16,358	1655,4	120603	121011	2610	-1224	1386	287
G04q	64	30,000	17	15,007	1685,7	120603	121011	3000	-1200	1800	266
Go1p	64	34,000	17	24,940	1757,4	120603	121011	2673	-837	1836	305
HAABl	64	20,955	17	24,096	1731,4	120605	121012	3780	-1450	2330	228
Skf01c	64	17,995	16	5,000	1282,6	120508	121008	3350	-1514	1836	221
Fl01c	64	26,004	15	55,322	1329,8	120508	121008	3180	-2035	1145	305
Oer					1830,0	130531		4405			

Appendix B: Balance distribution by elevation in 2011_12.

ΔS : area in elevation range, $\sum\Delta S$: cumulative area above given elevation, b_w: specific winter balance, b_s: specific summer balance. b_n: specific winter balance, ΔB_w : winter balance at a given elevation range, $\sum\Delta B_w$: cumulative winter balance above given elevation, ΔB_s summer balance at a given elevation range, $\sum\Delta B_s$: cumulative summer balance above given elevation, ΔB_n: net annual balance in a given elevation range, $\sum B_n$: cumulative net annual balance above given elevation.

Vatnajökull

Elevation (m a.s.l.)			**ΔS (km^2)**	**$\sum\Delta S$ (km^2)**	**b_w (mm)**	**b_s (mm)**	**b_n (mm)**	**ΔB_w (10^6m^3)**	**$\sum\Delta B_w$ (10^6m^3)**	**ΔB_s (10^6m^3)**	**$\sum\Delta B_s$ (10^6m^3)**	**ΔB_n (10^6m^3)**	**$\sum B_n$ (10^6m^3)**
2000	2050	2025	0,5	0,5	5453	-147	5306	2,6	3	0,0	0	2,5	3
1950	2000	1975	16,3	16,8	2728	-256	2472	44,5	47	-4,2	-4	40,3	43
1900	1950	1925	44,6	61,4	2720	-287	2433	121,5	169	-12,8	-17	108,6	152
1850	1900	1875	35,8	97,2	3097	-531	2566	111,2	280	-19,1	-36	92,1	244
1800	1850	1825	40,4	137,6	3478	-534	2943	140,7	421	-21,6	-58	119,1	363
1750	1800	1775	55,5	193,1	3018	-672	2345	168,2	589	-37,5	-95	130,7	493
1700	1750	1725	102,5	295,6	2738	-798	1940	281,4	870	-82,0	-177	199,4	693
1650	1700	1675	223,9	519,5	2783	-1032	1751	623,8	1494	-231,3	-409	392,5	1085
1600	1650	1625	355,2	874,7	2613	-1160	1453	928,8	2423	-412,2	-821	516,6	1602
1550	1600	1575	355,7	1230,4	2436	-1293	1142	867,0	3290	-460,3	-1281	406,7	2009
1500	1550	1525	418,4	1648,8	2299	-1469	830	962,4	4252	-614,9	-1896	347,5	2356
1450	1500	1475	450,3	2099,1	2252	-1632	620	1015,2	5267	-735,7	-2632	279,6	2636
1400	1450	1425	502,0	2601,1	2276	-1689	586	1143,6	6411	-849,0	-3481	294,6	2930
1350	1400	1375	537,1	3138,2	2186	-1686	499	1175,2	7586	-906,6	-4387	268,5	3199
1300	1350	1325	549,0	3687,2	2068	-1841	226	1136,9	8723	-1012,5	-5400	124,3	3323
1250	1300	1275	518,8	4206,0	1945	-2091	-146	1011,0	9734	-1087,1	-6487	-76,2	3247
1200	1250	1225	463,8	4669,8	1758	-2417	-658	817,6	10552	-1123,7	-7611	-306,1	2941
1150	1200	1175	411,2	5081,0	1592	-2684	-1092	656,8	11208	-1107,4	-8718	-450,6	2490
1100	1150	1125	367,9	5448,9	1499	-2904	-1405	553,3	11762	-1071,8	-9790	-518,5	1972
1050	1100	1075	331,3	5780,2	1381	-3151	-1770	459,3	12221	-1048,2	-10838	-588,9	1383
1000	1050	1025	306,2	6086,4	1218	-3436	-2217	374,9	12596	-1057,0	-11895	-682,1	701
950	1000	975	278,9	6365,3	1088	-3684	-2595	304,8	12901	-1031,4	-12927	-726,6	-26
900	950	925	239,7	6605,0	978	-3880	-2902	235,7	13136	-935,0	-13862	-699,3	-725
850	900	875	216,1	6821,1	831	-4068	-3236	180,7	13317	-884,0	-14746	-703,3	-1429
800	850	825	197,8	7018,9	721	-4256	-3535	143,7	13461	-848,2	-15594	-704,5	-2133
750	800	775	170,7	7189,6	615	-4457	-3841	105,2	13566	-761,6	-16355	-656,4	-2789
700	750	725	135,1	7324,7	645	-4475	-3830	87,2	13653	-605,1	-16960	-517,8	-3307
650	700	675	101,6	7426,3	635	-4389	-3754	64,8	13718	-447,8	-17408	-383,0	-3690
600	650	625	70,3	7496,6	637	-4361	-3723	45,0	13763	-308,2	-17716	-263,2	-3953
550	600	575	63,4	7560,0	541	-4511	-3969	34,7	13798	-288,4	-18005	-253,8	-4207
500	550	525	44,7	7604,7	465	-4761	-4296	21,0	13819	-215,3	-18220	-194,2	-4401
450	500	475	41,4	7646,1	366	-5090	-4723	15,3	13834	-212,8	-18433	-197,4	-4599
400	450	425	44,4	7690,5	246	-5415	-5168	11,1	13845	-243,2	-18676	-232,1	-4831
350	400	375	40,6	7731,1	-6	-5786	-5793	-0,3	13845	-238,4	-18915	-238,7	-5070
300	350	325	41,1	7772,2	-290	-6055	-6346	-12,1	13833	-252,4	-19167	-264,6	-5334
250	300	275	40,4	7812,6	-706	-6377	-7084	-28,8	13804	-260,3	-19427	-289,1	-5623
200	250	225	37,9	7850,5	-1227	-6810	-8037	-46,9	13757	-260,3	-19688	-307,2	-5931
150	200	175	31,6	7882,1	-1738	-7372	-9110	-55,4	13702	-234,9	-19922	-290,3	-6221
100	150	125	32,4	7914,5	-2170	-7853	-10024	-71,3	13630	-258,2	-20181	-329,5	-6550
50	100	75	24,7	7939,2	-2226	-7989	-10216	-56,4	13574	-202,5	-20383	-259,0	-6809
0	50	25	6,1	7945,3	-2043	-7917	-9960	-13,3	13561	-51,5	-20435	-64,7	-6874

Tungnaárjökull

Elevation (m a.s.l.)			ΔS (km^2)	$\sum\Delta S$ (km^2)	b_w (mm)	b_s (mm)	b_n (mm)	ΔB_w (10^6m^3)	$\sum\Delta B_w$ (10^6m^3)	ΔB_s (10^6m^3)	$\sum\Delta B_s$ (10^6m^3)	ΔB_n (10^6m^3)	$\sum B_n$ (10^6m^3)
1650	1700	1675	2,4	2,4	2701	-837	1863	6,4	6	-2,0	-2	4,4	4
1600	1650	1625	13,2	15,6	2563	-851	1712	33,8	40	-11,2	-13	22,5	27
1550	1600	1575	15,3	30,9	2444	-1074	1370	37,3	78	-16,4	-30	20,9	48
1500	1550	1525	15,3	46,2	2323	-1423	899	35,5	113	-21,8	-51	13,8	62
1450	1500	1475	18,5	64,7	2224	-1843	381	41,1	154	-34,0	-85	7,0	69
1400	1450	1425	23,3	88,0	2132	-2217	-84	49,7	204	-51,7	-137	-2,0	67
1350	1400	1375	21,7	109,7	2037	-2448	-410	44,1	248	-53,0	-190	-8,9	58
1300	1350	1325	28,1	137,8	1937	-2583	-646	54,3	302	-72,5	-263	-18,1	40
1250	1300	1275	21,8	159,6	1843	-2633	-789	40,2	343	-57,5	-320	-17,2	22
1200	1250	1225	24,0	183,6	1738	-2687	-948	41,8	384	-64,6	-385	-22,8	0
1150	1200	1175	21,0	204,6	1637	-2817	-1179	34,3	419	-59,0	-444	-24,7	-25
1100	1150	1125	19,2	223,8	1512	-3039	-1527	29,1	448	-58,5	-502	-29,4	-55
1050	1100	1075	20,0	243,8	1394	-3389	-1994	27,9	476	-67,8	-570	-39,9	-94
1000	1050	1025	18,2	262,0	1245	-3659	-2414	22,7	498	-66,6	-637	-43,9	-138
950	1000	975	18,9	280,9	1084	-3886	-2802	20,5	519	-73,4	-710	-52,9	-191
900	950	925	15,2	296,1	928	-4054	-3126	14,1	533	-61,5	-772	-47,5	-239
850	900	875	15,1	311,2	791	-4219	-3428	11,9	545	-63,6	-835	-51,7	-290
800	850	825	14,1	325,3	647	-4687	-4040	9,1	554	-66,0	-901	-56,9	-347
750	800	775	10,3	335,6	513	-5375	-4862	5,3	559	-55,2	-956	-49,9	-397
700	750	725	7,1	342,7	427	-5890	-5462	3,1	562	-42,1	-998	-39,1	-436
650	700	675	1,6	344,3	405	-5885	-5480	0,7	563	-9,9	-1008	-9,2	-445
600	650	625	0,0	344,3	385	-5839	-5454	0,0	563	-0,4	-1009	-0,3	-446

Sylgjujökull

Elevation (m a.s.l.)			ΔS (km^2)	$\sum\Delta S$ (km^2)	b_w (mm)	b_s (mm)	b_n (mm)	ΔB_w (10^6m^3)	$\sum\Delta B_w$ (10^6m^3)	ΔB_s (10^6m^3)	$\sum\Delta B_s$ (10^6m^3)	ΔB_n (10^6m^3)	$\sum B_n$ (10^6m^3)
1600	1650	1625	2,0	2,0	2404	-725	1679	4,8	5	-1,5	-2	3,4	3
1550	1600	1575	6,8	8,8	2287	-883	1403	15,4	20	-6,0	-7	9,5	13
1500	1550	1525	18,9	27,7	2041	-1182	859	38,5	59	-22,3	-30	16,2	29
1450	1500	1475	12,3	40,0	1958	-1785	172	24,1	83	-22,0	-52	2,1	31
1400	1450	1425	8,2	48,2	1945	-2232	-287	16,0	99	-18,3	-70	-2,4	29
1350	1400	1375	5,1	53,3	1928	-2446	-518	9,8	109	-12,4	-83	-2,6	26
1300	1350	1325	5,3	58,6	1864	-2584	-720	9,8	119	-13,6	-96	-3,8	22
1250	1300	1275	10,4	69,0	1775	-2649	-874	18,4	137	-27,4	-124	-9,0	13
1200	1250	1225	12,6	81,6	1641	-2712	-1071	20,6	158	-34,1	-158	-13,5	0
1150	1200	1175	14,4	96,0	1483	-2829	-1345	21,3	179	-40,7	-198	-19,3	-20
1100	1150	1125	13,2	109,2	1317	-3063	-1745	17,4	196	-40,4	-239	-23,0	-43
1050	1100	1075	13,4	122,6	1136	-3421	-2284	15,2	211	-45,8	-285	-30,6	-73
1000	1050	1025	9,3	131,9	1002	-3727	-2725	9,3	221	-34,6	-319	-25,3	-98
950	1000	975	3,1	135,0	998	-3931	-2932	3,1	224	-12,0	-331	-9,0	-107
900	950	925	1,6	136,6	943	-4158	-3214	1,5	225	-6,7	-338	-5,1	-113
850	900	875	0,2	136,8	892	-4312	-3420	0,2	226	-0,8	-339	-0,6	-113

Köldukvíslarjökul

Elevation (m a.s.l.)			ΔS (km^2)	$\sum\Delta S$ (km^2)	b_w (mm)	b_s (mm)	b_n (mm)	ΔB_w (10^6m^3)	$\sum\Delta B_w$ (10^6m^3)	ΔB_s (10^6m^3)	$\sum\Delta B_s$ (10^6m^3)	ΔB_n (10^6m^3)	$\sum B_n$ (10^6m^3)
1950	2000	1975	3,6	3,6	2474	-294	2179	8,9	9	-1,1	-1	7,8	8
1900	1950	1925	12,4	16,0	2565	-331	2233	31,8	41	-4,1	-5	27,7	36
1850	1900	1875	5,9	21,9	2516	-428	2087	14,7	55	-2,5	-8	12,2	48
1800	1850	1825	6,0	27,9	2460	-488	1972	14,7	70	-2,9	-11	11,8	60
1750	1800	1775	10,5	38,4	2499	-535	1963	26,3	96	-5,6	-16	20,7	80
1700	1750	1725	17,9	56,3	2375	-576	1798	42,4	139	-10,3	-27	32,1	112
1650	1700	1675	15,6	71,9	2218	-645	1573	34,6	173	-10,1	-37	24,5	137
1600	1650	1625	13,8	85,7	2086	-768	1318	28,8	202	-10,6	-47	18,2	155
1550	1600	1575	19,2	104,9	1984	-940	1043	38,2	240	-18,1	-65	20,1	175
1500	1550	1525	20,9	125,8	1829	-1196	633	38,2	279	-25,0	-90	13,2	188
1450	1500	1475	19,3	145,1	1746	-1449	296	33,7	312	-28,0	-118	5,7	194
1400	1450	1425	14,2	159,3	1670	-1617	52	23,8	336	-23,0	-141	0,7	195
1350	1400	1375	15,3	174,6	1596	-1756	-160	24,4	361	-26,8	-168	-2,4	192
1300	1350	1325	17,5	192,1	1494	-1938	-443	26,1	387	-33,9	-202	-7,8	185
1250	1300	1275	18,0	210,1	1371	-2148	-776	24,8	412	-38,9	-241	-14,1	171
1200	1250	1225	18,3	228,4	1213	-2433	-1219	22,2	434	-44,5	-285	-22,3	148
1150	1200	1175	16,4	244,8	1043	-2920	-1876	17,1	451	-47,9	-333	-30,8	118
1100	1150	1125	14,9	259,7	905	-3549	-2644	13,5	464	-53,1	-386	-39,5	78
1050	1100	1075	13,1	272,8	794	-4172	-3378	10,5	475	-54,9	-441	-44,5	34
1000	1050	1025	11,1	283,9	702	-4723	-4021	7,8	483	-52,5	-494	-44,7	-11
950	1000	975	10,5	294,4	628	-5090	-4461	6,6	489	-53,3	-547	-46,8	-58
900	950	925	5,6	300,0	579	-5278	-4698	3,3	493	-29,6	-577	-26,4	-84
850	900	875	0,5	300,5	549	-5306	-4756	0,3	493	-2,9	-580	-2,6	-87

Dyngjujökull

Elevation (m a.s.l.)			ΔS (km^2)	$\sum\Delta S$ (km^2)	b_w (mm)	b_s (mm)	b_n (mm)	ΔB_w (10^6m^3)	$\sum\Delta B_w$ (10^6m^3)	ΔB_s (10^6m^3)	$\sum\Delta B_s$ (10^6m^3)	ΔB_n (10^6m^3)	$\sum B_n$ (10^6m^3)
1950	2000	1975	7,4	7,4	2357	-241	2116	17,4	18	-1,8	-2	15,7	16
1900	1950	1925	23,2	30,6	2537	-252	2284	58,7	76	-5,8	-8	52,9	69
1850	1900	1875	15,9	46,5	2520	-685	1835	40,1	116	-10,9	-19	29,2	98
1800	1850	1825	9,7	56,2	2550	-843	1707	24,8	141	-8,2	-27	16,6	115
1750	1800	1775	16,0	72,2	2549	-930	1619	40,7	182	-14,9	-42	25,9	140
1700	1750	1725	27,3	99,5	2584	-996	1587	70,4	252	-27,1	-69	43,3	184
1650	1700	1675	71,6	171,1	2706	-1123	1582	193,7	446	-80,4	-149	113,3	297
1600	1650	1625	114,0	285,1	2560	-1258	1302	292,0	738	-143,5	-293	148,5	445
1550	1600	1575	94,7	379,8	2319	-1440	879	219,7	958	-136,4	-429	83,3	529
1500	1550	1525	89,7	469,5	2117	-1673	444	189,9	1148	-150,0	-579	39,8	569
1450	1500	1475	75,1	544,6	1893	-1985	-91	142,2	1290	-149,1	-728	-6,9	562
1400	1450	1425	61,4	606,0	1649	-2323	-673	101,3	1391	-142,6	-871	-41,3	520
1350	1400	1375	49,4	655,4	1380	-2643	-1263	68,2	1459	-130,6	-1001	-62,4	458
1300	1350	1325	37,9	693,3	1143	-2850	-1706	43,4	1503	-108,1	-1110	-64,7	393
1250	1300	1275	41,3	734,6	925	-3015	-2089	38,3	1541	-124,6	-1234	-86,4	307
1200	1250	1225	48,8	783,4	681	-3247	-2566	33,3	1574	-158,7	-1393	-125,4	181
1150	1200	1175	48,2	831,6	424	-3551	-3126	20,5	1595	-171,4	-1564	-150,9	30
1100	1150	1125	44,0	875,6	238	-3832	-3594	10,5	1605	-168,8	-1733	-158,2	-128
1050	1100	1075	33,1	908,7	136	-4076	-3940	4,5	1610	-135,2	-1868	-130,7	-259
1000	1050	1025	35,5	944,2	50	-4289	-4238	1,8	1612	-153,0	-2021	-151,2	-410
950	1000	975	30,8	975,0	-81	-4544	-4625	-2,5	1609	-140,1	-2161	-142,6	-552
900	950	925	25,6	1000,6	-230	-4816	-5046	-5,9	1603	-124,4	-2286	-130,3	-683
850	900	875	24,9	1025,5	-356	-5072	-5429	-9,0	1594	-128,8	-2415	-137,8	-820
800	850	825	19,7	1045,2	-457	-5328	-5785	-9,2	1585	-107,3	-2522	-116,5	-937
750	800	775	15,2	1060,4	-506	-5609	-6115	-7,5	1577	-83,6	-2605	-91,1	-1028
700	750	725	1,7	1062,1	-532	-5764	-6297	-0,7	1577	-7,8	-2613	-8,5	-1037

Brúarjökull

Elevation (m a.s.l.)			ΔS (km^2)	$\sum\Delta S$ (km^2)	b_w (mm)	b_s (mm)	b_n (mm)	ΔB_w ($10^6 m^3$)	$\sum\Delta B_w$ ($10^6 m^3$)	ΔB_s ($10^6 m^3$)	$\sum\Delta B_s$ ($10^6 m^3$)	ΔB_n ($10^6 m^3$)	$\sum B_n$ ($10^6 m^3$)
1850	1900	1875	0,8	0,8	2569	-582	1987	2,2	2	-0,5	-1	1,7	2
1800	1850	1825	4,2	5,0	2746	-482	2263	11,4	14	-2,0	-3	9,4	11
1750	1800	1775	3,0	8,0	2709	-564	2145	8,0	22	-1,7	-4	6,4	18
1700	1750	1725	3,7	11,7	2617	-715	1902	9,8	31	-2,7	-7	7,1	25
1650	1700	1675	5,3	17,0	2577	-925	1652	13,6	45	-4,9	-12	8,7	33
1600	1650	1625	44,4	61,4	2548	-1222	1326	113,3	158	-54,3	-66	59,0	92
1550	1600	1575	47,6	109,0	2443	-1349	1093	116,4	275	-64,3	-130	52,1	144
1500	1550	1525	69,8	178,8	2341	-1464	877	163,6	438	-102,3	-233	61,3	206
1450	1500	1475	73,9	252,7	2358	-1513	844	174,4	613	-111,9	-345	62,4	268
1400	1450	1425	108,1	360,8	2399	-1412	987	259,5	872	-152,7	-497	106,8	375
1350	1400	1375	148,2	509,0	2176	-1352	823	322,7	1195	-200,6	-698	122,2	497
1300	1350	1325	151,3	660,3	1856	-1512	344	281,0	1476	-228,9	-927	52,1	549
1250	1300	1275	144,8	805,1	1676	-1815	-139	242,8	1719	-263,0	-1190	-20,2	529
1200	1250	1225	121,8	926,9	1479	-2193	-713	180,2	1899	-267,2	-1457	-87,0	442
1150	1200	1175	105,8	1032,7	1300	-2403	-1102	137,6	2037	-254,3	-1711	-116,7	325
1100	1150	1125	86,8	1119,5	1143	-2535	-1392	99,2	2136	-220,1	-1931	-120,8	204
1050	1100	1075	73,3	1192,8	997	-2756	-1758	73,2	2209	-202,2	-2134	-129,0	75
1000	1050	1025	65,6	1258,4	824	-3152	-2327	54,1	2263	-206,9	-2340	-152,8	-77
950	1000	975	59,4	1317,8	657	-3608	-2951	39,0	2302	-214,2	-2555	-175,2	-253
900	950	925	48,9	1366,7	496	-4022	-3525	24,3	2326	-196,7	-2751	-172,4	-425
850	900	875	44,9	1411,6	337	-4354	-4016	15,1	2341	-195,4	-2947	-180,2	-605
800	850	825	41,4	1453,0	193	-4634	-4440	8,0	2350	-191,8	-3139	-183,8	-789
750	800	775	36,1	1489,1	60	-4925	-4865	2,2	2352	-177,9	-3316	-175,7	-965
700	750	725	23,8	1512,9	-24	-5143	-5167	-0,6	2351	-122,2	-3439	-122,7	-1088
650	700	675	12,8	1525,7	-75	-5337	-5413	-1,0	2350	-68,2	-3507	-69,1	-1157
600	650	625	0,3	1526,0	-73	-5384	-5457	0,0	2350	-1,8	-3509	-1,8	-1158

Eyjabakkajökull

Elevation (m a.s.l.)			ΔS (km^2)	$\sum\Delta S$ (km^2)	b_w (mm)	b_s (mm)	b_n (mm)	ΔB_w ($10^6 m^3$)	$\sum\Delta B_w$ ($10^6 m^3$)	ΔB_s ($10^6 m^3$)	$\sum\Delta B_s$ ($10^6 m^3$)	ΔB_n ($10^6 m^3$)	$\sum B_n$ ($10^6 m^3$)
1550	1600	1575	0,0	0,0	3998	-1011	2986	0,0	0	0,0	0	0,0	0
1500	1550	1525	0,0	0,0	4014	-982	3032	0,4	0	0,0	0	0,3	0
1450	1500	1475	1,0	1,0	3875	-1063	2812	3,8	4	-1,0	-1	2,7	3
1400	1450	1425	1,8	2,8	3780	-1118	2661	7,0	11	-2,1	-3	4,9	8
1350	1400	1375	2,5	5,3	3557	-1281	2276	9,0	20	-3,2	-6	5,8	14
1300	1350	1325	3,9	9,2	3317	-1495	1822	13,0	33	-5,8	-12	7,1	21
1250	1300	1275	13,4	22,6	2719	-1725	993	36,3	69	-23,1	-35	13,3	34
1200	1250	1225	13,3	35,9	2416	-1932	484	32,2	102	-25,7	-61	6,4	41
1150	1200	1175	14,7	50,6	2054	-2323	-269	30,2	132	-34,1	-95	-4,0	37
1100	1150	1125	12,3	62,9	1693	-2591	-897	20,8	153	-31,8	-127	-11,0	26
1050	1100	1075	10,6	73,5	1440	-2853	-1412	15,3	168	-30,2	-157	-15,0	11
1000	1050	1025	10,1	83,6	1243	-3179	-1935	12,6	180	-32,2	-189	-19,6	-9
950	1000	975	7,7	91,3	1033	-3540	-2507	8,0	188	-27,4	-217	-19,4	-28
900	950	925	5,2	96,5	862	-3903	-3041	4,5	193	-20,3	-237	-15,8	-44
850	900	875	3,9	100,4	762	-4160	-3397	3,0	196	-16,2	-253	-13,3	-57
800	850	825	3,2	103,6	682	-4373	-3690	2,2	198	-13,8	-267	-11,7	-69
750	800	775	3,4	107,0	567	-4657	-4090	1,9	200	-15,7	-283	-13,8	-83
700	750	725	3,3	110,3	404	-5073	-4668	1,3	201	-16,7	-300	-15,4	-98
650	700	675	1,7	112,0	290	-5343	-5053	0,5	202	-9,1	-309	-8,6	-107

Hoffellsjökull

Elevation (m a.s.l.)			ΔS (km^2)	∑ΔS (km^2)	b_w (mm)	b_s (mm)	b_n (mm)	ΔB_w ($10^6 m^3$)	$\sum\Delta B_w$ ($10^6 m^3$)	ΔB_s ($10^6 m^3$)	$\sum\Delta B_s$ ($10^6 m^3$)	ΔB_n ($10^6 m^3$)	$\sum B_n$ ($10^6 m^3$)
1450	1500	1475	0,9	0,9	3915	-964	2950	3,6	4	-0,9	-1	2,7	3
1400	1450	1425	6,7	7,6	3181	-1236	1945	21,3	25	-8,3	-9	13,0	16
1350	1400	1375	10,0	17,6	3023	-1330	1693	30,1	55	-13,3	-22	16,9	33
1300	1350	1325	15,4	33,0	2893	-1500	1392	44,4	100	-23,1	-46	21,4	54
1250	1300	1275	33,6	66,6	2765	-1710	1055	92,8	192	-57,4	-103	35,4	89
1200	1250	1225	26,8	93,4	2925	-1886	1039	78,4	271	-50,5	-153	27,9	117
1150	1200	1175	18,2	111,6	3059	-2051	1007	55,7	326	-37,4	-191	18,3	136
1100	1150	1125	17,5	129,1	3096	-2163	933	54,2	381	-37,8	-229	16,3	152
1050	1100	1075	13,6	142,7	2965	-2287	677	40,2	421	-31,0	-260	9,2	161
1000	1050	1025	10,0	152,7	2582	-2420	161	25,8	447	-24,2	-284	1,6	163
950	1000	975	9,0	161,7	2158	-2592	-434	19,5	466	-23,4	-307	-3,9	159
900	950	925	6,4	168,1	1858	-2791	-932	12,0	478	-18,0	-325	-6,0	153
850	900	875	4,3	172,4	1627	-2961	-1334	7,0	485	-12,8	-338	-5,8	147
800	850	825	3,5	175,9	1473	-3106	-1633	5,3	490	-11,2	-349	-5,9	141
750	800	775	3,8	179,7	1288	-3279	-1990	5,0	495	-12,7	-362	-7,7	134
700	750	725	3,8	183,5	1078	-3461	-2383	4,1	500	-13,3	-375	-9,1	124
650	700	675	3,4	186,9	899	-3651	-2751	3,0	503	-12,3	-387	-9,2	115
600	650	625	2,5	189,4	747	-3871	-3123	1,8	504	-9,6	-397	-7,7	107
550	600	575	1,8	191,2	644	-4076	-3431	1,2	506	-7,4	-404	-6,2	101
500	550	525	1,5	192,7	575	-4280	-3704	0,9	506	-6,3	-411	-5,5	96
450	500	475	0,9	193,6	499	-4526	-4027	0,5	507	-4,2	-415	-3,7	92
400	450	425	0,9	194,5	378	-4854	-4475	0,4	507	-4,6	-420	-4,3	88
350	400	375	0,6	195,1	166	-5251	-5084	0,0	507	-3,1	-423	-3,0	85
300	350	325	0,9	196,0	-57	-5603	-5661	0,0	507	-5,1	-428	-5,2	80
250	300	275	2,1	198,1	-345	-5947	-6292	-0,7	507	-12,9	-441	-13,7	66
200	250	225	3,3	201,4	-662	-6234	-6897	-2,2	504	-20,4	-461	-22,6	43
150	200	175	2,6	204,0	-1208	-6726	-7934	-3,1	501	-17,5	-479	-20,6	23
100	150	125	2,1	206,1	-1742	-7263	-9005	-3,7	498	-15,5	-494	-19,2	4
50	100	75	2,8	208,9	-2272	-7777	-10050	-6,4	491	-21,8	-516	-28,1	-25
0	50	25	0,5	209,4	-2491	-7880	-10371	-1,4	490	-4,4	-520	-5,8	-31

Breiðamerkurjökull

Elevation (m a.s.l.)			ΔS (km^2)	$\sum\Delta S$ (km^2)	b_w (mm)	b_s (mm)	b_n (mm)	ΔB_w (10^6m^3)	$\sum\Delta B_w$ (10^6m^3)	ΔB_s (10^6m^3)	$\sum\Delta B_s$ (10^6m^3)	ΔB_n (10^6m^3)	$\sum B_n$ (10^6m^3)
1900	1950	1925	0,0	0,0	5665	-154	5511	0,2	0	0,0	0	0,2	0
1850	1900	1875	0,4	0,4	5272	-198	5074	1,9	2	0,0	0	1,8	2
1800	1850	1825	0,4	0,8	4907	-266	4641	2,2	4	-0,1	0	2,1	4
1750	1800	1775	0,8	1,6	4465	-331	4134	3,7	8	-0,3	-1	3,4	8
1700	1750	1725	2,5	4,1	3525	-597	2927	8,7	17	-1,5	-2	7,2	15
1650	1700	1675	5,8	9,9	2930	-867	2063	16,9	34	-5,0	-7	11,9	27
1600	1650	1625	15,8	25,7	2668	-1072	1595	42,2	76	-17,0	-24	25,2	52
1550	1600	1575	25,7	51,4	2548	-1224	1324	65,6	141	-31,5	-55	34,1	86
1500	1550	1525	32,2	83,6	2503	-1351	1152	80,5	222	-43,5	-99	37,1	123
1450	1500	1475	44,3	127,9	2446	-1355	1091	108,3	330	-60,0	-159	48,3	171
1400	1450	1425	58,3	186,2	2397	-1405	992	139,9	470	-82,0	-241	57,9	229
1350	1400	1375	88,7	274,9	2368	-1398	969	210,0	680	-124,0	-365	86,0	315
1300	1350	1325	96,9	371,8	2395	-1606	789	232,2	912	-155,7	-521	76,5	392
1250	1300	1275	59,4	431,2	2372	-1974	397	141,0	1053	-117,4	-638	23,6	415
1200	1250	1225	39,7	470,9	2305	-2314	-8	91,5	1145	-91,8	-730	-0,3	415
1150	1200	1175	32,6	503,5	2202	-2566	-364	71,9	1217	-83,8	-814	-11,9	403
1100	1150	1125	27,7	531,2	2128	-2761	-632	59,0	1276	-76,5	-890	-17,5	386
1050	1100	1075	24,1	555,3	2012	-2890	-877	48,5	1324	-69,6	-960	-21,1	364
1000	1050	1025	22,1	577,4	1859	-3005	-1145	41,2	1365	-66,5	-1026	-25,4	339
950	1000	975	24,5	601,9	1718	-3151	-1433	42,1	1407	-77,3	-1103	-35,1	304
900	950	925	27,3	629,2	1630	-3272	-1641	44,6	1452	-89,6	-1193	-44,9	259
850	900	875	26,2	655,4	1501	-3408	-1906	39,3	1491	-89,3	-1282	-50,0	209
800	850	825	26,0	681,4	1358	-3543	-2184	35,4	1527	-92,4	-1375	-57,0	152
750	800	775	25,3	706,7	1165	-3699	-2534	29,4	1556	-93,5	-1468	-64,1	88
700	750	725	23,9	730,6	1040	-3789	-2749	24,9	1581	-90,7	-1559	-65,8	22
650	700	675	30,8	761,4	847	-3846	-2998	26,1	1607	-118,6	-1678	-92,5	-70
600	650	625	26,2	787,6	730	-4018	-3287	19,1	1626	-105,3	-1783	-86,1	-156
550	600	575	26,8	814,4	609	-4266	-3657	16,4	1643	-115,1	-1898	-98,7	-255
500	550	525	15,6	830,0	570	-4531	-3961	9,0	1652	-71,3	-1969	-62,4	-317
450	500	475	16,2	846,2	456	-4992	-4536	7,4	1659	-81,1	-2050	-73,7	-391
400	450	425	15,8	862,0	361	-5313	-4952	5,7	1665	-84,4	-2135	-78,6	-470
350	400	375	12,9	874,9	181	-5512	-5330	2,4	1667	-71,9	-2207	-69,5	-539
300	350	325	12,9	887,8	-112	-5617	-5729	-1,5	1666	-73,4	-2280	-74,8	-614
250	300	275	12,0	899,8	-567	-5874	-6441	-6,8	1659	-70,8	-2351	-77,6	-692
200	250	225	11,5	911,3	-1232	-6525	-7757	-14,2	1645	-75,0	-2426	-89,1	-781
150	200	175	8,5	919,8	-1744	-7221	-8966	-15,0	1630	-62,0	-2488	-76,9	-858
100	150	125	7,9	927,7	-1972	-7619	-9592	-15,5	1614	-60,0	-2548	-75,5	-933
50	100	75	6,0	933,7	-2056	-7814	-9870	-12,5	1602	-47,4	-2595	-59,9	-993
0	50	25	2,9	936,6	-2090	-7929	-10020	-6,4	1596	-24,3	-2619	-30,7	-1024

Síðujökull

Elevation (m a.s.l.)			ΔS (km^2)	$\sum\Delta S$ (km^2)	b_w (mm)	b_s (mm)	b_n (mm)	ΔB_w (10^6m^3)	$\sum\Delta B_w$ (10^6m^3)	ΔB_s (10^6m^3)	$\sum\Delta B_s$ (10^6m^3)	ΔB_n (10^6m^3)	$\sum B_n$ (10^6m^3)
1700	1750	1725	0,7	0,7	3462	-1456	2005	2,6	3	-1,1	-1	1,5	2
1650	1700	1675	5,2	5,9	3026	-1371	1654	15,6	18	-7,1	-8	8,5	10
1600	1650	1625	11,1	17,0	2673	-1194	1478	29,8	48	-13,3	-22	16,5	27
1550	1600	1575	10,1	27,1	2509	-1302	1206	25,3	73	-13,2	-35	12,2	39
1500	1550	1525	20,1	47,2	2377	-1476	901	47,9	121	-29,7	-64	18,2	57
1450	1500	1475	40,1	87,3	2266	-1860	405	90,9	212	-74,6	-139	16,3	73
1400	1450	1425	26,9	114,2	2160	-2125	35	58,1	270	-57,1	-196	1,0	74
1350	1400	1375	21,3	135,5	2044	-2382	-338	43,6	314	-50,8	-247	-7,2	67
1300	1350	1325	17,4	152,9	1962	-2552	-589	34,2	348	-44,5	-291	-10,3	57
1250	1300	1275	16,6	169,5	1910	-2638	-728	31,6	380	-43,7	-335	-12,1	45
1200	1250	1225	21,2	190,7	1857	-2756	-899	39,3	419	-58,4	-394	-19,0	25
1150	1200	1175	18,1	208,8	1756	-3049	-1292	31,8	451	-55,2	-449	-23,4	2
1100	1150	1125	17,0	225,8	1627	-3298	-1670	27,7	478	-56,1	-505	-28,4	-26
1050	1100	1075	18,0	243,8	1466	-3555	-2088	26,4	505	-64,0	-569	-37,6	-64
1000	1050	1025	21,8	265,6	1289	-3807	-2517	28,1	533	-82,9	-652	-54,8	-119
950	1000	975	21,8	287,4	1113	-4013	-2900	24,3	557	-87,6	-739	-63,3	-182
900	950	925	22,1	309,5	991	-4148	-3157	21,9	579	-91,8	-831	-69,9	-252
850	900	875	20,9	330,4	916	-4246	-3329	19,1	598	-88,6	-920	-69,5	-322
800	850	825	25,0	355,4	841	-4364	-3522	21,0	619	-109,1	-1029	-88,0	-410
750	800	775	25,5	380,9	741	-4503	-3761	18,9	638	-114,8	-1144	-95,9	-505
700	750	725	26,0	406,9	584	-4646	-4061	15,2	653	-120,7	-1264	-105,5	-611
650	700	675	15,8	422,7	476	-4797	-4320	7,5	661	-75,9	-1340	-68,4	-679
600	650	625	7,4	430,1	411	-4948	-4536	3,1	664	-36,7	-1377	-33,6	-713
550	600	575	0,2	430,3	392	-5087	-4694	0,0	664	-1,1	-1378	-1,0	-714

Skaftárjökull

Elevation (m a.s.l.)			ΔS (km^2)	$\sum\Delta S$ (km^2)	b_w (mm)	b_s (mm)	b_n (mm)	ΔB_w (10^6m^3)	$\sum\Delta B_w$ (10^6m^3)	ΔB_s (10^6m^3)	$\sum\Delta B_s$ (10^6m^3)	ΔB_n (10^6m^3)	$\sum B_n$ (10^6m^3)
1350	1400	1375	2,4	2,4	2031	-2432	-401	4,9	5	-5,9	-6	-1,0	-1
1300	1350	1325	5,5	7,9	1958	-2562	-603	10,7	16	-14,0	-20	-3,3	-4
1250	1300	1275	4,5	12,4	1878	-2651	-772	8,5	24	-12,0	-32	-3,5	-8
1200	1250	1225	6,5	18,9	1801	-2777	-976	11,6	36	-17,9	-50	-6,3	-14
1150	1200	1175	9,3	28,2	1700	-3013	-1312	15,7	52	-27,9	-78	-12,1	-26
1100	1150	1125	12,3	40,5	1573	-3260	-1687	19,3	71	-39,9	-118	-20,7	-47
1050	1100	1075	14,2	54,7	1422	-3531	-2108	20,2	91	-50,0	-168	-29,9	-77
1000	1050	1025	12,1	66,8	1255	-3776	-2521	15,2	106	-45,7	-213	-30,5	-107
950	1000	975	7,6	74,4	1091	-3962	-2870	8,3	114	-30,1	-244	-21,8	-129
900	950	925	5,3	79,7	969	-4090	-3120	5,2	120	-21,8	-265	-16,6	-146
850	900	875	5,6	85,3	865	-4214	-3348	4,8	124	-23,4	-289	-18,6	-164
800	850	825	5,7	91,0	755	-4365	-3609	4,4	129	-25,5	-314	-21,1	-185
750	800	775	5,1	96,1	671	-4490	-3818	3,4	132	-23,0	-337	-19,6	-205
700	750	725	3,6	99,7	582	-4686	-4103	2,1	134	-16,7	-354	-14,6	-220
650	700	675	2,8	102,5	556	-4849	-4293	1,6	136	-13,7	-368	-12,1	-232
600	650	625	0,8	103,3	485	-5016	-4530	0,4	136	-3,9	-371	-3,5	-235

Vestari Skaftárketill

Elevation (m a.s.l.)			ΔS (km^2)	$\sum\Delta S$ (km^2)	b_w (mm)	b_s (mm)	b_n (mm)	ΔB_w (10^6m^3)	$\sum\Delta B_w$ (10^6m^3)	ΔB_s (10^6m^3)	$\sum\Delta B_s$ (10^6m^3)	ΔB_n (10^6m^3)	$\sum B_n$ (10^6m^3)
1900	1950	1925	0,7	0,7	2680	-343	2337	1,8	2	-0,2	0	1,6	2
1850	1900	1875	0,6	1,3	2680	-425	2254	1,6	3	-0,2	-1	1,3	3
1800	1850	1825	0,7	2,0	2672	-530	2142	2,0	5	-0,4	-1	1,6	5
1750	1800	1775	2,7	4,7	2631	-652	1979	7,1	13	-1,8	-3	5,3	10
1700	1750	1725	5,9	10,6	2515	-636	1878	14,8	27	-3,7	-6	11,0	21
1650	1700	1675	6,7	17,3	2402	-614	1788	16,0	43	-4,1	-11	11,9	33
1600	1650	1625	7,4	24,7	2338	-646	1691	17,3	61	-4,8	-15	12,5	45
1550	1600	1575	5,2	29,9	2242	-725	1516	11,6	72	-3,7	-19	7,8	53
1500	1550	1525	1,5	31,4	2215	-759	1456	3,3	75	-1,1	-20	2,1	55

Eystri Skaftárketill

Elevation (m a.s.l.)			ΔS (km^2)	$\sum\Delta S$ (km^2)	b_w (mm)	b_s (mm)	b_n (mm)	ΔB_w (10^6m^3)	$\sum\Delta B_w$ (10^6m^3)	ΔB_s (10^6m^3)	$\sum\Delta B_s$ (10^6m^3)	ΔB_n (10^6m^3)	$\sum B_n$ (10^6m^3)
1750	1800	1775	1,1	1,1	2645	-727	1917	2,9	3	-0,8	-1	2,1	2
1700	1750	1725	11,1	12,2	2631	-747	1883	29,3	32	-8,3	-9	21,0	23
1650	1700	1675	16,2	28,4	2690	-773	1917	43,6	76	-12,5	-22	31,0	54
1600	1650	1625	9,2	37,6	2570	-699	1871	23,8	100	-6,5	-28	17,3	71
1550	1600	1575	2,2	39,8	2560	-691	1869	5,7	105	-1,5	-30	4,1	76

Gjálp

Elevation (m a.s.l.)			ΔS (km^2)	$\sum\Delta S$ (km^2)	b_w (mm)	b_s (mm)	b_n (mm)	ΔB_w (10^6m^3)	$\sum\Delta B_w$ (10^6m^3)	ΔB_s (10^6m^3)	$\sum\Delta B_s$ (10^6m^3)	ΔB_n (10^6m^3)	$\sum B_n$ (10^6m^3)
1900	1950	1925	0,5	0,5	2680	-331	2348	1,5	2	-0,2	0	1,3	1
1850	1900	1875	0,6	1,1	2680	-502	2177	1,7	3	-0,3	-1	1,4	3
1800	1850	1825	1,2	2,3	2676	-681	1994	3,1	6	-0,8	-1	2,3	5
1750	1800	1775	4,5	6,8	2669	-784	1885	12,1	18	-3,6	-5	8,6	14
1700	1750	1725	15,9	22,7	2752	-893	1859	43,9	62	-14,2	-19	29,6	43
1650	1700	1675	16,5	39,2	2916	-1014	1902	48,2	110	-16,8	-36	31,4	75
1600	1650	1625	0,0	39,2	2940	-1017	1923	0,0	111	0,0	-36	0,0	75

Grímsvötn

Elevation (m a.s.l.)			ΔS (km^2)	$\sum\Delta S$ (km^2)	b_w (mm)	b_s (mm)	b_n (mm)	ΔB_w (10^6m^3)	$\sum\Delta B_w$ (10^6m^3)	ΔB_s (10^6m^3)	$\sum\Delta B_s$ (10^6m^3)	ΔB_n (10^6m^3)	$\sum B_n$ (10^6m^3)
1700	1750	1725	0,8	0,8	2990	-1147	1842	2,5	3	-0,9	-1	1,5	2
1650	1700	1675	40,8	41,6	2975	-1162	1813	121,5	124	-47,5	-48	74,1	76
1600	1650	1625	30,6	72,2	2917	-1231	1685	89,4	213	-37,7	-86	51,6	127
1550	1600	1575	18,6	90,8	2940	-1402	1538	54,8	268	-26,1	-112	28,7	156
1500	1550	1525	16,9	107,7	2940	-1719	1221	49,6	318	-29,0	-141	20,6	177
1450	1500	1475	11,6	119,3	2969	-2161	808	34,4	352	-25,0	-166	9,4	186
1400	1450	1425	15,1	134,4	2981	-2552	429	44,9	397	-38,4	-205	6,5	192
1350	1400	1375	0,6	135,0	2793	-1918	875	1,8	399	-1,2	-206	0,6	193

Appendix C: Coordinates at velocity measurement stakes.

Position of velocity measurement stakes determined by GPS sub-metre differential (I), fast static (FS) and kinematic (K).
(Accuracy of horizontal position 0.5 – 1.0 m, and vertical accuracy 1-2 m for DGPS, about 1cm for fast static, and 3 cm for kinematic).
The station Hofn in Höfn í Hornafirði is used as a stationary reference for all measurements, ÍSN93 datum, h_l is elevation above ellipsoid, dL antenna height, N estimated difference between ellipsoid and sea-level, H elevation in metres above sea level (H= h_l+N+dL). X and Y are ÍSN93 Lambert conformal conic projected coordinates. M is a quality marker.

Site	time	Date	#	Calender Day	Year	Latitude		Longitude		h_l (m a. e.)	dL (m)	N (m)	H (m a. s. l.)	X	Y	M
B07r	17,463	7	5	128	2012	64	25,79757	16	17,44054	1424,5	0,0	-67,1	1357,4	630486,45	439248,12	K
B07r	10,929	8	10	282	2012	64	25,79740	16	17,43953	1420,4	0,0	-67,1	1353,4	630487,27	439247,83	K
B09s	11,321	10	5	131	2012	64	45,04250	16	5,47275	824,1	0,0	-66,7	757,4	638441,75	475394,18	K
B09s	9,479	10	10	284	2012	64	45,04248	16	5,47243	818,4	0,0	-66,7	751,7	638442,00	475394,16	K
B10s	13,629	10	5	131	2012	64	43,68500	16	6,70096	878,4	0,0	-66,7	811,7	637583,36	472829,89	K
B10s	9,962	10	10	284	2012	64	43,68528	16	6,70063	872,8	0,0	-66,7	806,1	637583,60	472830,43	K
B11b	10,796	10	5	131	2012	64	40,94350	16	10,48892	1028,8	0,0	-66,8	962,0	634805,66	467605,37	K
B11b	19,700	9	10	283	2012	64	40,94751	16	10,48535	1026,3	0,0	-66,8	959,5	634808,17	467612,95	K
B12r	10,188	10	5	131	2012	64	38,27283	16	14,12847	1144,0	0,0	-66,9	1077,1	632130,06	462520,06	K
B12r	19,125	9	10	283	2012	64	38,28110	16	14,12126	1140,5	0,0	-66,9	1073,6	632135,13	462535,66	K
B13r	16,096	9	5	130	2012	64	34,52229	16	19,76067	1281,6	0,0	-67,0	1214,6	627940,58	455364,91	K
B13r	17,254	9	10	283	2012	64	34,53215	16	19,74874	1277,6	0,0	-67,0	1210,6	627949,32	455383,62	K
B13a25b	12,000	10	5	132	2012	64	34,12888	16	16,74807	1283,0	-1,5	-67,0	1214,5	630375,91	454737,20	*
B13a25b	15,442	9	10	283	2012	64	34,13847	16	16,73936	1277,8	0,0	-67,0	1210,8	630382,10	454755,30	K
B13n25b	12,000	10	5	132	2012	64	35,67245	16	18,09513	1247,5	-1,5	-67,0	1179,0	629178,48	457556,73	*
B13n25b	18,458	9	10	283	2012	64	35,68237	16	18,08630	1240,7	0,0	-67,0	1173,7	629184,66	457575,14	K
B13n5b	12,000	10	5	132	2012	64	36,77303	16	16,39702	1209,1	-1,5	-67,0	1140,6	630444,26	459657,52	*
B13n5b	18,792	9	10	283	2012	64	36,78148	16	16,38785	1202,3	0,0	-66,9	1135,3	630450,89	459673,54	K
B13v25b	10,946	10	5	131	2012	64	34,85227	16	22,87416	1300,1	0,0	-67,1	1233,0	625430,70	455873,49	K
B13v25b	16,475	9	10	283	2012	64	34,86253	16	22,85991	1296,4	0,0	-67,1	1229,4	625441,29	455893,00	K
B14s	10,963	10	10	284	2012	64	31,66102	16	24,66195	1376,4	0,0	-67,1	1309,3	624247,10	449890,34	K
B14t	17,154	10	5	131	2012	64	31,63961	16	24,69616	1381,4	0,0	-67,1	1314,3	624221,38	449849,48	K
B14t	11,029	10	10	284	2012	64	31,64726	16	24,68214	1376,9	0,0	-67,1	1309,8	624232,01	449864,13	K
B15g	17,883	10	5	131	2012	64	28,48452	16	30,00705	1466,3	0,0	-67,2	1399,1	620207,43	443820,96	K
B15g	11,450	10	10	284	2012	64	28,48927	16	29,99478	1461,6	0,0	-67,2	1394,4	620216,91	443830,17	K
B16t	16,108	7	5	128	2012	64	23,56930	16	42,06554	1591,2	0,0	-67,3	1523,9	610879,98	434327,71	K
B16t	12,000	14	10	288	2012	64	23,56857	16	42,06715	1589,7	0,0	-67,3	1522,4	610878,74	434326,31	K
B17r	16,754	9	5	130	2012	64	36,73679	16	28,80213	1279,5	0,0	-67,1	1212,4	620561,53	459179,80	K
B17r	17,092	9	10	283	2012	64	36,74359	16	28,79729	1276,3	0,0	-67,1	1209,2	620564,89	459192,58	K
B18p	14,950	8	5	129	2012	64	31,57779	16	0,10823	1378,4	0,0	-66,9	1311,4	643880,01	450603,70	K
B18p	15,646	8	10	282	2012	64	31,58302	16	0,11078	1373,8	0,0	-66,9	1306,9	643877,50	450613,32	K
B19p	12,913	8	5	129	2012	64	27,93272	15	55,16967	1499,5	0,0	-66,9	1432,7	648156,74	444029,12	K
B19p	12,967	8	10	282	2012	64	27,93251	15	55,16929	1492,4	0,0	-66,9	1425,5	648157,06	444028,74	K
BB0q	9,129	8	5	129	2012	64	22,71745	16	5,05086	1586,3	0,0	-66,9	1519,4	640688,71	433973,79	K
BB0q	11,125	8	10	282	2012	64	22,71699	16	5,05206	1582,1	-1,0	-66,9	1514,2	640687,78	433972,91	K
BORag	12,538	3	6	155	2012	64	24,93749	17	20,14722	1470,4	0,0	-67,7	1402,7	580209,16	435909,33	K
BORag	12,683	13	10	287	2012	64	24,93382	17	20,14890	1479,8	0,0	-67,7	1412,1	580207,99	435902,49	K
BORTHNb	14,175	6	5	127	2012	64	25,10254	17	19,14765	1470,1	0,0	-67,7	1402,4	581003,74	436237,14	K
BORTHNb	16,471	13	10	287	2012	64	25,09902	17	19,14848	1491,4	-5,9	-67,7	1417,8	581003,25	436230,58	K
Br1g	17,713	20	4	111	2012	64	5,52034	16	19,48472	177,0	-0,7	-65,8	110,5	630440,47	401536,46	I
Br2i	16,794	20	4	111	2012	64	6,40253	16	22,54732	306,8	-0,7	-66,0	240,1	627885,11	403069,88	I
Br2j	17,243	20	4	111	2012	64	6,40355	16	22,54753	307,9	-0,7	-66,0	241,2	627884,86	403071,77	I
Br3O	15,987	20	4	111	2012	64	8,53076	16	24,13681	472,5	-0,7	-66,3	405,5	626432,39	406967,56	I
Br4C	14,463	20	4	111	2012	64	11,75717	16	22,12384	639,2	-0,7	-66,5	572,0	627814,88	413024,69	I
Br7p	18,163	7	5	128	2012	64	22,14303	16	16,95057	1315,1	0,0	-67,0	1248,1	631171,30	432481,13	K
Br7p	10,513	8	10	282	2012	64	22,12028	16	16,94597	1308,9	0,0	-67,0	1241,9	631176,82	432439,06	K
Bruq	13,833	9	5	130	2012	64	40,99814	15	55,22226	848,1	0,0	-66,7	781,3	646932,50	468273,76	K
Bruq	16,633	8	10	282	2012	64	40,99810	15	55,22211	841,9	0,0	-66,7	775,1	646932,62	468273,71	K
Budq	14,550	9	5	130	2012	64	35,98916	15	59,89779	1201,9	0,0	-66,9	1135,0	643659,16	458798,76	K
Budq	16,254	8	10	282	2012	64	35,99810	15	59,89581	1197,8	0,0	-66,9	1130,9	643659,95	458815,42	K
D05p	11,429	7	5	128	2012	64	42,21849	16	54,62802	1268,7	0,0	-67,4	1201,4	599640,28	468608,43	K
D05p	13,304	13	10	287	2012	64	42,22523	16	54,61729	1265,8	0,0	-67,4	1198,4	599648,39	468621,23	K

D07p	12,288	7	5	128	2012	64	38,28623	16	59,24106	1436,7	0,0	-67,5	1369,2	596207,86	461187,04	K
D07p	12,754	13	10	287	2012	64	38,29825	16	59,22967	1432,0	0,0	-67,5	1364,5	596216,22	461209,65	K
D09o	13,413	7	5	128	2012	64	31,80069	17	0,55146	1648,2	0,0	-67,6	1580,6	595543,63	449109,85	K
D09o	12,263	13	10	287	2012	64	31,80481	17	0,55295	1644,1	0,0	-67,6	1576,5	595542,20	449117,47	K
D12p	14,646	7	5	128	2012	64	28,98497	17	0,13809	1715,3	0,0	-67,6	1647,7	596039,46	443891,30	K
D12p	16,696	10	10	284	2012	64	28,98555	17	0,13783	1711,4	0,0	-67,6	1643,8	596039,64	443892,38	K
E01q	12,463	9	5	130	2012	64	41,51554	15	33,40906	750,2	0,0	-66,7	683,5	664209,45	470128,50	K
E01q	17,354	8	10	282	2012	64	41,51569	15	33,40847	744,1	0,0	-66,7	677,5	664209,90	470128,80	K
E02q	11,813	9	5	130	2012	64	39,13767	15	35,96986	1021,7	0,0	-66,8	955,0	662413,50	465606,62	K
E02q	18,142	8	10	282	2012	64	39,14537	15	35,96555	1016,4	0,0	-66,8	949,6	662416,16	465621,09	K
E03r	11,521	9	5	130	2012	64	36,66802	15	36,90978	1252,8	0,0	-66,9	1186,0	661911,59	460984,45	K
E03r	17,742	8	10	282	2012	64	36,67178	15	36,91200	1248,9	0,0	-66,9	1182,1	661909,45	460991,32	K
E04q	10,763	9	5	130	2012	64	34,95029	15	37,09592	1355,7	0,0	-66,8	1288,9	661933,98	457789,54	K
E04q	17,333	8	10	282	2012	64	34,95082	15	37,09581	1351,0	0,0	-66,8	1284,1	661934,01	457790,53	K
Fl01c	14,075	8	5	129	2012	64	26,00387	15	55,32206	1396,6	0,0	-66,8	1329,8	648209,10	440443,62	K
Fl01c	12,125	8	10	282	2012	64	25,99600	15	55,30463	1392,2	0,0	-66,8	1325,4	648223,79	440429,69	K
G02i	14,733	3	6	155	2012	64	26,85836	17	17,72021	1628,7	0,0	-67,7	1561,0	582062,01	439528,95	K
G02i	13,329	11	10	285	2012	64	26,85497	17	17,72314	1624,9	0,0	-67,7	1557,1	582059,83	439522,59	K
G03j	15,696	3	6	155	2012	64	28,44938	17	16,35790	1723,2	0,0	-67,7	1655,4	583074,00	442513,64	K
G03j	13,942	11	10	285	2012	64	28,44781	17	16,35945	1720,0	0,0	-67,7	1652,3	583072,84	442510,68	K
G04q	16,375	3	6	155	2012	64	30,00007	17	15,00682	1753,4	0,0	-67,7	1685,7	584076,94	445423,49	K
G04q	14,225	11	10	285	2012	64	30,00036	17	15,00634	1750,1	0,0	-67,7	1682,4	584077,31	445424,04	K
gb2rorb	15,417	8	5	129	2012	64	34,09299	16	0,02071	1267,0	0,0	-66,9	1200,1	643728,29	455274,99	K
gb2rorb	13,300	9	10	283	2012	64	34,10051	16	0,02286	1267,6	0,0	-66,9	1200,7	643725,91	455288,86	K
gb2c	15,417	8	5	129	2012	64	34,09299	16	0,02071	1267,0	-1,0	-66,9	1199,1	643728,29	455274,99	K
gb2c	13,300	9	10	283	2012	64	34,10051	16	0,02286	1267,6	-4,6	-66,9	1196,1	643725,91	455288,86	K
Go1p	17,608	3	6	155	2012	64	33,99950	17	24,94003	1825,3	0,0	-67,8	1757,4	575938,11	452642,31	K
Go1p	15,042	11	10	285	2012	64	33,99866	17	24,93790	1824,3	0,0	-67,8	1756,4	575939,86	452640,80	K
HAABl	15,488	5	6	157	2012	64	20,95472	17	24,09551	1798,9	0,0	-67,5	1731,4	577225,37	428429,85	K
HAABl	10,363	12	10	286	2012	64	20,95474	17	24,09490	1795,1	0,0	-67,5	1727,6	577225,86	428429,91	K
Hof01j	17,083	8	5	129	2012	64	32,32683	15	35,83823	1207,0	0,0	-66,7	1140,3	663198,99	452976,08	K
Hof01j	10,133	9	10	283	2012	64	32,32103	15	35,83790	1202,3	0,0	-66,7	1135,6	663199,83	452965,33	K
K01s	15,117	5	5	126	2012	64	35,35041	17	52,77226	1040,6	0,0	-67,6	973,0	553662,83	454676,25	K
K01s	11,021	12	10	286	2012	64	35,35129	17	52,77467	1034,6	0,0	-67,6	967,0	553660,87	454677,85	K
K02t	15,592	5	5	126	2012	64	34,81689	17	49,68754	1248,3	0,0	-67,6	1180,6	556143,22	453729,78	K
K02t	10,788	12	10	286	2012	64	34,81840	17	49,69770	1244,4	0,0	-67,6	1176,8	556135,06	453732,45	K
K03s	16,325	5	5	126	2012	64	34,24454	17	46,37731	1367,0	0,0	-67,7	1299,4	558806,70	452716,71	K
K03s	10,475	12	10	286	2012	64	34,24625	17	46,39075	1363,2	0,0	-67,7	1295,6	558795,89	452719,68	K
K04t	16,642	5	5	126	2012	64	33,21059	17	42,24684	1556,0	0,0	-67,7	1488,3	562144,86	450861,88	K
K04t	10,113	12	10	286	2012	64	33,21336	17	42,26751	1551,8	0,0	-67,7	1484,1	562128,24	450866,67	K
K05t	18,042	5	5	126	2012	64	33,45121	17	35,42976	1748,7	0,0	-67,8	1680,9	567582,64	451425,42	K
K05t	17,808	11	10	285	2012	64	33,44830	17	35,44272	1743,8	0,0	-67,8	1676,0	567572,40	451419,78	K
K06s	20,075	3	6	155	2012	64	38,35086	17	31,36245	2036,3	0,0	-67,9	1968,4	570619,65	460600,69	K
K06s	15,875	11	10	285	2012	64	38,35041	17	31,36040	2036,9	-2,1	-67,9	1966,9	570621,31	460599,88	K
K07o	11,408	11	5	132	2012	64	29,12184	17	42,02508	1602,8	0,0	-67,7	1535,1	562478,24	443270,24	K
K07o	18,583	11	10	285	2012	64	29,12170	17	42,02612	1600,3	0,0	-67,7	1532,6	562477,42	443269,96	K
S01h	11,296	5	5	126	2012	64	7,00403	17	49,99005	814,4	0,0	-66,8	747,5	556855,47	402057,51	K
S01h	15,679	12	10	286	2012	64	7,00385	17	49,99097	805,7	0,0	-66,8	738,9	556854,73	402057,17	K
S02k	11,817	5	5	126	2012	64	12,15598	17	48,97769	1078,3	0,0	-67,0	1011,3	557498,29	411643,63	K
S02k	15,075	12	10	286	2012	64	12,14716	17	48,98061	1070,6	0,0	-67,0	1003,5	557496,23	411627,21	K
S04l	12,283	5	5	126	2012	64	16,20040	17	48,22708	1228,2	0,0	-67,2	1161,0	557963,70	419168,34	K
S04l	14,692	12	10	286	2012	64	16,18981	17	48,23910	1222,8	0,0	-67,2	1155,6	557954,37	419148,48	K

Salt	8,529	7	5	128	2012	64	24,39707	17	16,25130	1781,0	0,0	-67,7	1713,3	583365,35	434989,60	K
Skf01c	10,496	8	5	129	2012	64	17,99544	16	4,99971	1349,3	0,0	-66,6	1282,6	641134,46	425211,50	K
Skf01c	9,625	8	10	282	2012	64	17,99285	16	4,98548	1344,8	0,0	-66,6	1278,2	641146,14	425207,22	K
T01nn	11,571	4	5	125	2012	64	19,48437	18	8,22934	823,5	0,0	-67,3	756,3	541727,83	425006,35	K
T01nn	12,658	12	10	286	2012	64	19,48477	18	8,22937	816,6	0,0	-67,3	749,3	541727,80	425007,11	K
T02no	11,771	4	5	125	2012	64	19,60449	18	3,94823	1015,8	0,0	-67,3	948,6	545174,92	425278,56	K
T02no	12,329	12	10	286	2012	64	19,60438	18	3,95331	1009,8	0,0	-67,3	942,5	545170,83	425278,29	K
T03no	13,125	4	5	125	2012	64	20,20362	17	58,58780	1146,3	0,0	-67,3	1079,0	549476,78	426458,49	K
T03no	14,510	12	10	286	2012	64	20,20186	17	58,59690	1142,3	0,0	-67,3	1075,0	549469,50	426455,12	K
T04no	15,683	4	5	125	2012	64	21,33856	17	51,49947	1291,0	0,0	-67,4	1223,6	555148,82	428664,68	K
T04no	13,358	12	10	286	2012	64	21,33570	17	51,50972	1286,4	0,0	-67,4	1219,1	555140,67	428659,22	K
T05nn	16,854	4	5	125	2012	64	22,29796	17	42,97156	1412,2	-0,2	-67,5	1344,5	561977,44	430578,59	K
T05nn	17,033	12	10	286	2012	64	22,29565	17	42,98141	1412,6	-5,0	-67,5	1340,1	561969,60	430574,15	K
T05rorf	16,854	4	5	125	2012	64	22,29796	17	42,97156	1412,2	0,0	-67,5	1344,7	561977,44	430578,59	K
T05rorf	17,033	12	10	286	2012	64	22,29565	17	42,98141	1412,6	0,0	-67,5	1345,1	561969,60	430574,15	K
T06no	19,171	4	5	125	2012	64	24,28673	17	36,53088	1532,0	0,0	-67,6	1464,4	567077,53	434382,47	K
T06no	11,271	12	10	286	2012	64	24,28285	17	36,54162	1529,0	-1,6	-67,6	1459,7	567069,05	434375,09	K
T07nm	20,192	5	5	126	2012	64	25,30093	17	31,19279	1631,7	0,0	-67,7	1564,0	571322,45	436363,76	K
T07nm	18,583	12	10	286	2012	64	25,29872	17	31,20110	1627,4	0,0	-67,7	1559,7	571315,87	436359,51	K
T07rorj	20,296	5	5	126	2012	64	25,29708	17	31,20585	1631,3	-2,0	-67,7	1561,6	571312,13	436356,36	K
T07rorj	19,175	12	10	286	2012	64	25,29468	17	31,21333	1629,9	-1,0	-67,7	1561,2	571306,23	436351,76	K
T07rork	19,175	12	10	286	2012	64	25,29468	17	31,21333	1629,9	0,0	-67,7	1562,2	571306,23	436351,76	K
T08no	19,471	5	5	126	2012	64	26,30711	17	27,77800	1705,0	0,0	-67,8	1637,2	574018,93	438298,13	K
T08no	17,742	12	10	286	2012	64	26,30710	17	27,77908	1701,0	0,0	-67,8	1633,3	574018,07	438298,09	K

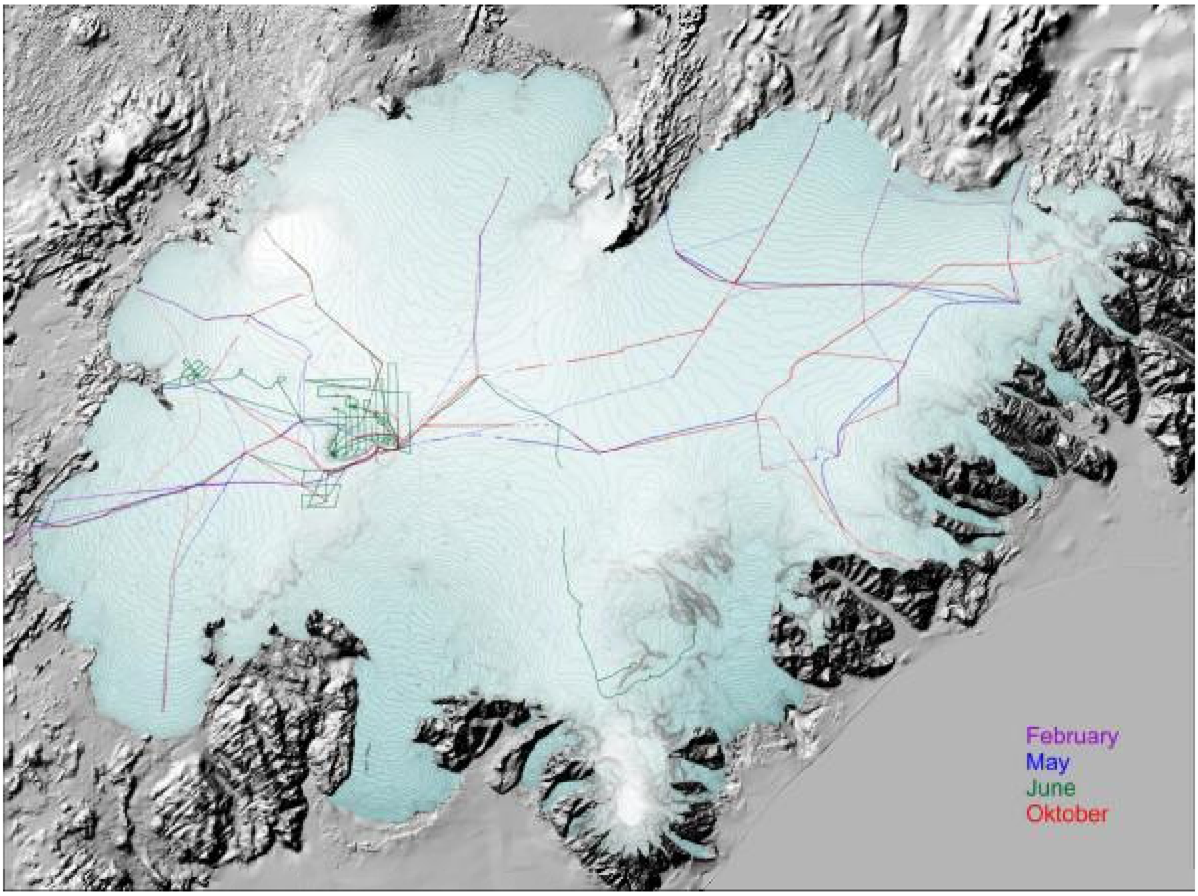

Surface elevation profiles surveyed with kinematic GPS (accuracy <10cm) in 2012.

Appendix D: Measured surface velocity on Vatnajökull in 2013.

	Calendar day		Calendar day		# of	translation		velocity	
Site	date	#	date	#	days	(m)	(°)	(cm/day)	(m/annum)
B07r	120507	128	121008	282	154	0,87	111	0,56	2,06
B09s	120510	131	121010	284	153	0,26	98	0,17	0,61
B10s	111021	294	120510	131	202	0,40	47	0,20	0,73
B10s	120510	131	121010	284	153	0,58	27	0,38	1,39
B10s	121010	284	130506	126	207	5,79	3	2,80	10,21
B11b	111021	294	120510	131	202	0,44	80	0,22	0,80
B11b	120510	131	121009	283	152	7,95	21	5,23	19,09
B12r	120510	131	121009	283	152	16,36	21	10,76	39,28
B13r	120509	130	121009	283	153	20,60	28	13,46	49,13
B13a25b	120510	132	121009	283	151	19,07	21	12,63	46,11
B13n25b	120510	132	121009	283	151	19,68	21	13,03	47,56
B13n5b	120510	132	121009	283	151	17,27	25	11,44	41,75
B13v25b	120510	131	121009	283	152	22,15	31	14,57	53,18
B14s	110506	126	121010	284	523	39,19	38	7,49	27,35
B14t	120510	131	121010	284	153	18,07	38	11,81	43,10
B15g	120510	131	121010	284	153	13,19	48	8,62	31,47
B16t	120507	128	121014	288	160	1,87	224	1,17	4,27
B17r	120509	130	121009	283	153	13,17	17	8,61	31,42
B18p	120508	129	121008	282	153	9,90	348	6,47	23,61
B19p	120508	129	121008	282	153	0,49	142	0,32	1,18
BB0q	120508	129	121008	282	153	1,29	229	0,84	3,07
BORag	120603	155	121013	287	132	6,93	191	5,25	19,16
BORTHNb	111022	295	120506	127	197	7,15	181	3,63	13,25
BORTHNb	120506	127	121013	287	160	6,55	186	4,10	14,95
BORTHNb	121013	287	131006	279	357	9,95	194	2,79	10,17
Br3O	120420	111	130131	31	285	21,79	145	7,65	27,91
Br4C	120420	111	130130	30	284	41,78	182	14,71	53,70
Br7p	120507	128	121008	282	154	42,30	175	27,46	100,25
Bruq	120509	130	121008	282	152	0,14	122	0,09	0,34
Budq	120509	130	121008	282	152	16,63	5	10,94	39,94
D05p	120507	128	121013	287	159	15,12	34	9,51	34,70
D07p	120507	128	121013	287	159	24,04	22	15,12	55,18
D09o	120507	128	121013	287	159	7,72	351	4,86	17,73
D12p	120507	128	121010	284	156	1,09	11	0,70	2,56
E01q	120509	130	121008	282	152	0,55	59	0,36	1,31
E02q	120509	130	121008	282	152	14,67	14	9,65	35,22
E03r	120509	130	121008	282	152	7,18	346	4,73	17,25
E04q	120509	130	121008	282	152	0,99	5	0,65	2,37
Fl01c	120508	129	121008	282	153	20,20	136	13,20	48,19
G02i	120603	155	121011	285	130	6,70	201	5,16	18,82
G03j	120603	155	121011	285	130	3,16	203	2,43	8,88
G04q	120603	155	121011	285	130	0,66	36	0,51	1,85
gb2rorb	111020	293	120508	129	201	11,26	354	5,60	20,44
gb2rorb	120508	129	121009	283	154	14,03	353	9,11	33,26
gb2rorb	121009	283	130507	127	209	10,95	355	5,24	19,12

Go1p	120603	155	121011	285	130	2,31	132	1,77	6,47
HAABl	120605	157	121012	286	129	0,49	86	0,38	1,39
Hof01j	120508	129	121009	283	154	10,74	179	6,98	25,47
K01s	120505	126	121012	286	160	2,52	310	1,58	5,75
K02t	120505	126	121012	286	160	8,58	289	5,36	19,57
K03s	120505	126	121012	286	160	11,19	286	6,99	25,52
K04t	120505	126	121012	286	160	17,29	287	10,81	39,45
K05t	120505	126	121011	285	159	11,67	243	7,34	26,79
K06s	120603	155	121011	285	130	1,83	117	1,41	5,15
K07o	120511	132	121011	285	153	0,87	253	0,57	2,08
S01h	120505	126	121012	286	160	0,82	246	0,51	1,87
S02k	120505	126	121012	286	160	16,50	188	10,32	37,65
S04l	120505	126	121012	286	160	21,88	206	13,68	49,92
Skf01c	120508	129	121008	282	153	12,44	113	8,13	29,67
T01nn	111023	296	120504	125	194	0,98	216	0,51	1,84
T01nn	120504	125	121012	286	161	0,74	358	0,46	1,68
T01nn	121012	286	130501	121	200	2,13	213	1,07	3,89
T02no	120504	125	121012	286	161	4,10	267	2,55	9,29
T03no	120504	125	121012	286	161	8,02	246	4,98	18,18
T04no	120504	125	121012	286	161	9,80	237	6,09	22,22
T05nn	120504	125	121012	286	161	9,00	242	5,59	20,41
T05nn	121012	286	131005	278	357	19,18	237	5,37	19,61
T05rorf	111023	296	120504	125	194	9,57	237	4,93	18,01
T05rorf	120504	125	121012	286	161	9,00	242	5,59	20,41
T05rorf	121012	286	130502	122	201	9,69	240	4,82	17,60
T06no	120504	125	121012	286	161	11,23	230	6,97	25,46
T07nm	120505	126	121012	286	160	7,83	238	4,89	17,86
T07rorj	111023	296	120505	126	195	9,37	244	4,80	17,54
T07rorj	120505	126	121012	286	160	7,47	233	4,67	17,04
T07rorl	121012	286	131005	278	357	15,79	241	4,42	16,14
T08no	120505	126	121012	286	160	0,87	269	0,54	1,98

Appendix E: Melt water runoff to selected rivers in summer 2012, derived from summer balance.

ΔS: area in a given elevation range where summer balance is negative, **$\sum\Delta S$**: cumulative area above a given elevation, **ΔQ_s**: melt water runoff from a given elevation range, **$\sum\Delta Q_s$** : cumulative melt water runoff from an area above given elevation.

Tungnaá water drainage basin

Elevation (m a. s. l.)		ΔS km^2	$\sum\Delta S$ km^2	ΔQ_s $(10^6 m^3)$	$\sum\Delta Q_s$ $(10^6 m^3)$
1350	1400	0,6	0,6	1,4	1,4
1300	1350	6,2	6,8	16,0	17,5
1250	1300	10,7	17,5	28,0	45,5
1200	1250	11,4	28,9	30,3	75,8
1150	1200	10,8	39,7	29,8	105,5
1100	1150	12,8	52,5	38,3	143,8
1050	1100	11,9	64,4	40,3	184,1
1000	1050	9,7	74,1	35,1	219,3
950	1000	10,8	84,9	41,5	260,8
900	950	9,0	93,9	36,6	297,4
850	900	8,3	102,2	35,8	333,1
800	850	8,6	110,8	41,7	374,8
750	800	6,3	117,1	35,7	410,5
700	750	4,2	121,3	25,8	436,3
650	700	0,5	121,8	3,5	439,9

Sylgja water drainage basin

Elevation (m a. s. l.)		ΔS km^2	$\sum\Delta S$ km^2	ΔQ_s $(10^6 m^3)$	$\sum\Delta Q_s$ $(10^6 m^3)$
1300	1350	1,3	1,3	3,5	3,5
1250	1300	3,6	4,9	9,7	13,2
1200	1250	6,4	11,3	17,5	30,6
1150	1200	8,3	19,6	23,4	54,0
1100	1150	6,6	26,2	19,9	73,9
1050	1100	7,6	33,8	25,7	99,7
1000	1050	3,8	37,6	14,2	113,8
950	1000	1,5	39,1	5,9	119,7
900	950	0,6	39,7	2,4	122,1
850	900	0,0	39,7	0,0	122,2

Western Skaftá cauldron water drainage basin

Elevation (m a. s. l.)		ΔS km^2	$\sum\Delta S$ km^2	ΔQ_s $(10^6 m^3)$	$\sum\Delta Q_s$ $(10^6 m^3)$
1700	1750	3,2	3,2	2,0	2,0
1650	1700	7,0	10,2	4,4	6,4
1600	1650	8,4	18,6	5,5	11,9
1550	1600	5,0	23,6	3,7	15,6
1500	1550	1,5	25,1	1,1	16,7

Eastern Skaftár cauldoron water drainage basin

Elevation (m a. s. l.)		ΔS km^2	$\Sigma\Delta S$ km^2	ΔQ_s (10^6m^3)	$\Sigma\Delta Q_s$ (10^6m^3)
1750	1800	2,5	2,5	1,7	1,7
1700	1750	10,6	13,1	7,9	9,6
1650	1700	14,8	27,9	11,5	21,2
1600	1650	9,3	37,2	6,5	27,7
1550	1600	2,2	39,4	1,5	29,2

Grímsvötn water drainage basin

Elevation (m a. s. l.)		ΔS km^2	$\Sigma\Delta S$ km^2	ΔQ_s (10^6m^3)	$\Sigma\Delta Q_s$ (10^6m^3)
1900	1950	0,6	0,6	0,2	0,2
1850	1900	1,3	1,9	0,6	0,8
1800	1850	1,6	3,5	1,0	1,8
1750	1800	3,9	7,4	3,0	4,9
1700	1750	15,9	23,3	14,3	19,1
1650	1700	56,4	79,7	63,1	82,3
1600	1650	30,9	110,6	38,0	120,3
1550	1600	18,7	129,3	26,2	146,5
1500	1550	16,7	146,0	28,7	175,2
1450	1500	11,6	157,6	25,0	200,2
1400	1450	15,1	172,7	38,4	238,7
1350	1400	0,6	173,3	1,2	239,9

Kaldakvísl water drainage basin

Elevation (m a. s. l.)		ΔS km^2	$\Sigma\Delta S$ km^2	ΔQ_s (10^6m^3)	$\Sigma\Delta Q_s$ (10^6m^3)
1950	2000	4,8	4,8	1,4	1,4
1900	1950	12,9	17,7	4,3	5,7
1850	1900	6,4	24,1	2,8	8,5
1800	1850	6,4	30,5	3,2	11,7
1750	1800	11,7	42,2	6,4	18,1
1700	1750	21,1	63,3	12,4	30,5
1650	1700	16,7	80,0	10,8	41,2
1600	1650	14,2	94,2	10,9	52,1
1550	1600	19,4	113,6	18,3	70,4
1500	1550	27,2	140,8	33,1	103,5
1450	1500	28,5	169,3	43,9	147,4
1400	1450	23,1	192,4	41,8	189,3
1350	1400	21,6	214,0	41,5	230,8
1300	1350	21,3	235,3	43,1	273,9
1250	1300	22,6	257,9	50,5	324,4
1200	1250	22,6	280,5	56,4	380,8
1150	1200	20,2	300,7	59,0	439,8
1100	1150	18,3	319,0	63,5	503,3
1050	1100	17,2	336,2	69,0	572,3
1000	1050	14,9	351,1	66,8	639,1
950	1000	10,7	361,8	54,0	693,1
900	950	5,6	367,4	29,6	722,7
850	900	0,5	367,9	2,9	725,6

Jökulsá á Fjöllum water drainage basin

Elevation (m a. s. l.)		ΔS km^2	ΣΔS km^2	ΔQ$_s$ (10^{6}m^3)	ΣΔQ$_s$ (10^{6}m^3)
2000	2050	0,0	0,0	0,0	0,0
1950	2000	8,2	8,2	2,0	2,0
1900	1950	25,6	33,8	6,7	8,7
1850	1900	18,4	52,2	12,4	21,1
1800	1850	14,6	66,8	11,0	32,1
1750	1800	22,3	89,1	19,1	51,2
1700	1750	34,2	123,3	32,5	83,7
1650	1700	79,5	202,8	88,4	172,1
1600	1650	116,5	319,3	145,9	318,1
1550	1600	100,9	420,2	144,2	462,2
1500	1550	97,8	518,0	162,3	624,5
1450	1500	85,7	603,7	168,5	792,9
1400	1450	74,3	678,0	171,9	964,9
1350	1400	60,2	738,2	158,3	1123,2
1300	1350	49,1	787,3	139,1	1262,3
1250	1300	52,5	839,8	157,8	1420,1
1200	1250	57,4	897,2	185,8	1606,0
1150	1200	54,5	951,7	192,4	1798,3
1100	1150	45,9	997,6	175,8	1974,2
1050	1100	34,1	1031,7	138,9	2113,0
1000	1050	36,4	1068,1	156,0	2269,0
950	1000	31,5	1099,6	142,9	2411,9
900	950	26,2	1125,8	126,3	2538,1
850	900	25,4	1151,2	128,9	2667,1
800	850	20,2	1171,4	107,9	2774,9
750	800	15,2	1186,6	85,1	2860,0
700	750	1,7	1188,3	10,0	2870,0

Kreppa and Kverká water drainage basin

Elevation (m a. s. l.)		ΔS km^2	$\sum\Delta S$ km^2	ΔQ_s ($10^6 m^3$)	$\sum\Delta Q_s$ ($10^6 m^3$)
1900	1950	0,0	0,0	0,0	0,0
1850	1900	1,0	1,0	0,6	0,6
1800	1850	4,3	5,3	2,1	2,7
1750	1800	2,8	8,1	1,6	4,3
1700	1750	3,6	11,7	2,6	6,9
1650	1700	5,0	16,7	4,6	11,5
1600	1650	37,9	54,6	46,0	57,5
1550	1600	22,6	77,2	30,5	88,0
1500	1550	14,3	91,5	20,8	108,8
1450	1500	15,4	106,9	23,4	132,2
1400	1450	19,3	126,2	29,9	162,0
1350	1400	25,2	151,4	39,5	201,5
1300	1350	20,5	171,9	33,8	235,3
1250	1300	16,4	188,3	31,1	266,4
1200	1250	18,1	206,4	40,8	307,2
1150	1200	18,2	224,6	44,8	352,0
1100	1150	17,5	242,1	45,6	397,6
1050	1100	11,6	253,7	32,5	430,1
1000	1050	14,1	267,8	44,8	474,9
950	1000	16,1	283,9	58,1	533,0
900	950	14,4	298,3	58,0	591,1
850	900	14,5	312,8	63,8	654,9
800	850	11,5	324,3	53,4	708,2
750	800	9,3	333,6	46,0	754,2
700	750	4,2	337,8	21,6	775,8
650	700	0,4	338,2	2,3	778,1

Jökulsá á Brú water drainage basin

Elevation (m a. s. l.)		ΔS km^2	$\sum\Delta S$ km^2	ΔQ_s ($10^6 m^3$)	$\sum\Delta Q_s$ ($10^6 m^3$)
1600	1650	8,3	8,3	10,3	10,3
1550	1600	30,4	38,7	41,1	51,4
1500	1550	60,6	99,3	88,8	140,1
1450	1500	63,6	162,9	96,8	236,9
1400	1450	95,6	258,5	133,2	370,2
1350	1400	124,5	383,0	162,9	533,0
1300	1350	133,2	516,2	198,4	731,4
1250	1300	128,3	644,5	231,5	963,0
1200	1250	102,8	747,3	224,5	1187,5
1150	1200	87,3	834,6	208,6	1396,1
1100	1150	69,3	903,9	174,3	1570,4
1050	1100	61,8	965,7	170,0	1740,4
1000	1050	51,8	1017,5	162,9	1903,3
950	1000	43,4	1060,9	156,4	2059,8
900	950	34,6	1095,5	139,0	2198,8
850	900	30,4	1125,9	131,6	2330,4
800	850	29,9	1155,8	138,4	2468,8
750	800	26,8	1182,6	131,9	2600,7
700	750	19,6	1202,2	100,6	2701,3
650	700	12,3	1214,5	65,8	2767,2
600	650	0,3	1214,8	1,8	2768,9

Jökulsá á Fljótsdal water drainage basin

Elevation (m a. s. l.)		ΔS km^2	$\sum\Delta S$ km^2	ΔQ_s $(10^6 m^3)$	$\sum\Delta Q_s$ $(10^6 m^3)$
1500	1550	0,0	0,0	0,0	0,0
1450	1500	0,9	0,9	1,0	1,1
1400	1450	1,9	2,8	2,1	3,2
1350	1400	2,8	5,6	3,7	6,9
1300	1350	5,2	10,8	7,9	14,8
1250	1300	15,8	26,6	27,3	42,2
1200	1250	15,9	42,5	30,8	72,9
1150	1200	17,6	60,1	40,5	113,4
1100	1150	15,1	75,2	39,0	152,4
1050	1100	12,7	87,9	36,3	188,7
1000	1050	11,9	99,8	37,9	226,7
950	1000	9,0	108,8	31,6	258,3
900	950	5,8	114,6	22,3	280,5
850	900	4,3	118,9	17,8	298,3
800	850	3,3	122,2	14,3	312,6
750	800	3,4	125,6	15,7	328,4
700	750	3,3	128,9	16,7	345,1
650	700	1,7	130,6	9,1	354,2

Hornafjarðarfljót water drainage basin

Elevation (m a. s. l.)		ΔS km^2	$\sum\Delta S$ km^2	ΔQ_s (10^6m^3)	$\sum\Delta Q_s$ (10^6m^3)
1450	1500	1,0	1,0	0,9	0,9
1400	1450	7,4	8,4	9,6	10,5
1350	1400	12,2	20,6	17,2	27,7
1300	1350	18,3	38,9	29,0	56,8
1250	1300	36,6	75,5	63,3	120,1
1200	1250	30,2	105,7	57,1	177,2
1150	1200	20,8	126,5	42,9	220,1
1100	1150	19,8	146,3	43,0	263,0
1050	1100	15,3	161,6	35,2	298,3
1000	1050	11,7	173,3	28,5	326,8
950	1000	11,1	184,4	28,9	355,7
900	950	8,2	192,6	23,0	378,6
850	900	5,5	198,1	16,4	395,1
800	850	4,4	202,5	13,7	408,8
750	800	4,1	206,6	13,5	422,3
700	750	4,0	210,6	13,7	436,1
650	700	3,5	214,1	12,6	448,7
600	650	2,6	216,7	10,0	458,7
550	600	2,0	218,7	8,2	466,9
500	550	1,8	220,5	7,8	474,7
450	500	1,4	221,9	6,5	481,2
400	450	1,3	223,2	6,2	487,4
350	400	0,8	224,0	4,1	491,5
300	350	1,1	225,1	6,3	497,7
250	300	2,3	227,4	14,0	511,7
200	250	3,5	230,9	21,8	533,5
150	200	2,7	233,6	18,1	551,5
100	150	2,1	235,7	15,6	567,1
50	100	2,8	238,5	21,8	588,9
0	50	0,6	239,1	4,4	593,3

Jökulsá á Breiðamerkursandi water drainage basin

Elevation (m a. s. l.)		ΔS km^2	$\sum\Delta S$ km^2	ΔQ_s $(10^6 m^3)$	$\sum\Delta Q_s$ $(10^6 m^3)$
1700	1750	0,8	0,8	0,8	0,8
1650	1700	4,0	4,8	4,1	4,8
1600	1650	12,9	17,7	14,8	19,6
1550	1600	19,1	36,8	23,9	43,5
1500	1550	23,0	59,8	31,7	75,3
1450	1500	35,2	95,0	47,1	122,3
1400	1450	49,6	144,6	68,9	191,2
1350	1400	83,3	227,9	115,6	306,8
1300	1350	85,4	313,3	135,3	442,1
1250	1300	53,1	366,4	105,0	547,1
1200	1250	35,1	401,5	81,3	628,4
1150	1200	28,9	430,4	74,1	702,5
1100	1150	24,6	455,0	67,8	770,3
1050	1100	20,7	475,7	59,8	830,1
1000	1050	17,8	493,5	53,9	884,1
950	1000	19,0	512,5	59,9	944,0
900	950	20,2	532,7	66,1	1010,1
850	900	20,5	553,2	69,9	1080,0
800	850	20,2	573,4	71,1	1151,1
750	800	19,5	592,9	72,0	1223,1
700	750	21,1	614,0	79,4	1302,5
650	700	26,7	640,7	101,5	1404,0
600	650	18,5	659,2	74,2	1478,2
550	600	18,5	677,7	79,2	1557,3
500	550	7,0	684,7	31,7	1589,0
450	500	7,7	692,4	38,9	1627,9
400	450	5,8	698,2	31,2	1659,1
350	400	5,5	703,7	30,0	1689,1
300	350	6,5	710,2	36,3	1725,4
250	300	6,0	716,2	34,9	1760,3
200	250	6,3	722,5	41,5	1801,9
150	200	5,1	727,6	37,5	1839,4
100	150	5,1	732,7	39,2	1878,6
50	100	4,1	736,8	32,2	1910,8
0	50	2,7	739,5	21,2	1932,0

Breiðárlón/Fjallsárlón water drainage basin

Elevation (m a. s. l.)		ΔS km^2	$\sum\Delta S$ km^2	ΔQ_s ($10^6 m^3$)	$\sum\Delta Q_s$ ($10^6 m^3$)
1950	2000	0,6	0,6	0,0	0,0
1900	1950	0,8	1,4	0,1	0,2
1850	1900	1,5	2,9	0,3	0,5
1800	1850	2,1	5,0	0,6	1,1
1750	1800	2,5	7,5	0,9	1,9
1700	1750	2,9	10,4	1,3	3,2
1650	1700	2,9	13,3	1,5	4,7
1600	1650	4,0	17,3	2,7	7,4
1550	1600	4,2	21,5	3,4	10,8
1500	1550	6,0	27,5	5,8	16,6
1450	1500	5,0	32,5	5,5	22,2
1400	1450	5,3	37,8	6,8	29,0
1350	1400	6,4	44,2	10,1	39,1
1300	1350	12,6	56,8	22,3	61,4
1250	1300	6,7	63,5	13,5	74,9
1200	1250	5,6	69,1	12,9	87,8
1150	1200	5,1	74,2	13,1	100,9
1100	1150	4,5	78,7	12,5	113,4
1050	1100	5,0	83,7	14,4	127,8
1000	1050	6,0	89,7	17,8	145,6
950	1000	7,0	96,7	21,9	167,5
900	950	8,4	105,1	27,5	194,9
850	900	6,7	111,8	23,0	217,9
800	850	8,4	120,2	29,8	247,7
750	800	8,8	129,0	32,8	280,5
700	750	6,1	135,1	23,4	304,0
650	700	7,4	142,5	29,1	333,1
600	650	8,3	150,8	33,7	366,8
550	600	8,8	159,6	37,5	404,3
500	550	9,5	169,1	42,8	447,0
450	500	9,6	178,7	46,9	494,0
400	450	11,1	189,8	58,1	552,1
350	400	8,5	198,3	46,7	598,8
300	350	7,7	206,0	43,0	641,8
250	300	7,4	213,4	44,0	685,8
200	250	6,8	220,2	44,0	729,8
150	200	4,6	224,8	32,8	762,6
100	150	4,3	229,1	32,5	795,2
50	100	3,7	232,8	28,5	823,7
0	50	1,8	234,6	14,3	838,0

Skeiðarársandur water drainage basin (Gígja)

Elevation (m a. s. l.)		ΔS km^2	$\sum\Delta S$ km^2	ΔQ_s $(10^6 m^3)$	$\sum\Delta Q_s$ $(10^6 m^3)$
1700	1750	1,2	1,2	1,4	1,4
1650	1700	20,5	21,7	25,2	26,6
1600	1650	76,2	97,9	94,5	121,1
1550	1600	84,6	182,5	112,9	234,0
1500	1550	104,1	286,6	151,3	385,4
1450	1500	97,6	384,2	148,0	533,4
1400	1450	95,1	479,3	146,5	679,9
1350	1400	83,3	562,6	132,1	812,0
1300	1350	71,9	634,5	122,0	934,1
1250	1300	62,8	697,3	120,7	1054,8
1200	1250	52,9	750,2	120,2	1174,9
1150	1200	44,9	795,1	117,5	1292,4
1100	1150	36,1	831,2	103,7	1396,1
1050	1100	29,5	860,7	91,6	1487,7
1000	1050	25,0	885,7	81,8	1569,4
950	1000	25,0	910,7	85,6	1655,1
900	950	24,8	935,5	89,8	1744,8
850	900	27,8	963,3	105,2	1850,1
800	850	22,5	985,8	88,1	1938,2
750	800	19,6	1005,4	79,7	2017,9
700	750	19,1	1024,5	82,1	2100,0
650	700	11,9	1036,4	53,7	2153,8
600	650	13,1	1049,5	61,4	2215,2
550	600	12,4	1061,9	60,0	2275,2
500	550	8,3	1070,2	42,0	2317,2
450	500	5,5	1075,7	29,8	2347,1
400	450	6,7	1082,4	38,8	2385,8
350	400	11,1	1093,5	68,0	2453,8
300	350	14,2	1107,7	93,2	2547,0
250	300	15,3	1123,0	105,4	2652,4
200	250	12,4	1135,4	90,9	2743,3
150	200	11,3	1146,7	87,5	2830,8
100	150	13,5	1160,2	110,2	2941,0
50	100	5,0	1165,2	42,5	2983,5

Súla water drainage basin

Elevation (m a. s. l.)		ΔS km^2	$\sum\Delta S$ km^2	ΔQ_s (10^6m^3)	$\sum\Delta Q_s$ (10^6m^3)
1700	1750	0,5	0,5	0,8	0,8
1650	1700	1,4	1,9	2,2	3,0
1600	1650	2,6	4,5	4,2	7,2
1550	1600	4,1	8,6	7,2	14,4
1500	1550	5,9	14,5	10,9	25,3
1450	1500	11,4	25,9	22,3	47,6
1400	1450	11,1	37,0	22,9	70,4
1350	1400	9,3	46,3	20,5	90,9
1300	1350	8,2	54,5	18,9	109,8
1250	1300	6,7	61,2	16,3	126,1
1200	1250	8,1	69,3	20,5	146,6
1150	1200	9,2	78,5	24,5	171,1
1100	1150	15,6	94,1	44,4	215,5
1050	1100	15,9	110,0	49,5	265,0
1000	1050	16,5	126,5	55,0	320,0
950	1000	18,7	145,2	66,0	386,0
900	950	15,3	160,5	56,9	442,9
850	900	12,1	172,6	46,8	489,7
800	850	11,7	184,3	46,2	535,9
750	800	7,0	191,3	28,9	564,8
700	750	6,0	197,3	26,5	591,2
650	700	4,9	202,2	22,4	613,7
600	650	9,0	211,2	42,3	655,9
550	600	11,7	222,9	56,8	712,8
500	550	8,9	231,8	45,2	757,9
450	500	7,2	239,0	38,5	796,4
400	450	6,3	245,3	36,0	832,4
350	400	4,8	250,1	29,4	861,8
300	350	1,8	251,9	12,0	873,8
250	300	0,9	252,8	6,7	880,5
200	250	0,8	253,6	5,8	886,2
150	200	0,8	254,4	6,3	892,5
100	150	0,8	255,2	6,9	899,4
50	100	0,6	255,8	5,6	904,9

Djúpá water drainage basin

Elevation (m a. s. l.)		ΔS km^2	$\Sigma\Delta S$ km^2	ΔQ_s $(10^6 m^3)$	$\Sigma\Delta Q_s$ $(10^6 m^3)$
1450	1500	0,1	0,1	0,3	0,3
1400	1450	0,3	0,4	0,8	1,1
1350	1400	0,9	1,3	2,3	3,4
1300	1350	3,8	5,1	9,9	13,2
1250	1300	3,3	8,4	9,0	22,2
1200	1250	2,9	11,3	8,2	30,5
1150	1200	3,5	14,8	10,4	40,9
1100	1150	5,3	20,1	16,6	57,5
1050	1100	7,0	27,1	24,3	81,8
1000	1050	9,8	36,9	36,9	118,7
950	1000	8,0	44,9	32,2	151,0
900	950	8,1	53,0	33,8	184,8
850	900	7,5	60,5	32,2	217,0
800	850	9,1	69,6	40,0	257,0
750	800	6,7	76,3	30,2	287,1
700	750	4,0	80,3	18,6	305,7
650	700	3,0	83,3	14,0	319,8
600	650	0,4	83,7	2,0	321,8

Brunná water drainage basin

Elevation (m a. s. l.)		ΔS km^2	$\Sigma\Delta S$ km^2	ΔQ_s $(10^6 m^3)$	$\Sigma\Delta Q_s$ $(10^6 m^3)$
1050	1100	0,0	0,0	0,3	0,3
1000	1050	1,1	1,1	4,4	4,6
950	1000	3,3	4,4	13,3	17,9
900	950	4,2	8,6	17,2	35,1
850	900	4,3	12,9	18,3	53,4
800	850	4,9	17,8	21,2	74,6
750	800	5,4	23,2	24,4	99,0
700	750	6,4	29,6	29,5	128,5
650	700	3,9	33,5	18,7	147,2
600	650	2,3	35,8	11,7	158,9
550	600	0,0	35,8	0,2	159,0

Hverfisfljót water drainage basin

Elevation (m a. s. l.)		**ΔS km^2**	**$\Sigma\Delta S$ km^2**	**ΔQ_s ($10^6 m^3$)**	**$\Sigma\Delta Q_s$ ($10^6 m^3$)**
1700	1750	0,8	0,8	1,2	1,2
1650	1700	5,1	5,9	7,0	8,2
1600	1650	9,1	15,0	11,3	19,5
1550	1600	9,0	24,0	12,0	31,4
1500	1550	19,7	43,7	29,3	60,7
1450	1500	42,0	85,7	78,7	139,4
1400	1450	28,5	114,2	60,8	200,2
1350	1400	24,5	138,7	58,3	258,5
1300	1350	22,9	161,6	58,3	316,8
1250	1300	18,6	180,2	48,9	365,6
1200	1250	20,2	200,4	55,6	421,2
1150	1200	14,1	214,5	43,2	464,4
1100	1150	10,9	225,4	36,4	500,8
1050	1100	10,2	235,6	36,5	537,3
1000	1050	9,3	244,9	35,5	572,7
950	1000	9,4	254,3	37,8	610,5
900	950	8,9	263,2	36,9	647,5
850	900	7,4	270,6	31,3	678,8
800	850	9,3	279,9	40,5	719,3
750	800	11,5	291,4	51,7	771,0
700	750	13,7	305,1	63,6	834,6
650	700	7,8	312,9	37,7	872,3
600	650	4,6	317,5	22,6	894,9
550	600	0,2	317,7	0,9	895,8

Skaftá water drainage basin

Elevation (m a. s. l.)		**ΔS km^2**	**$\Sigma\Delta S$ km^2**	**ΔQ_s ($10^6 m^3$)**	**$\Sigma\Delta Q_s$ ($10^6 m^3$)**
1650	1700	2,9	2,9	2,4	2,4
1600	1650	16,1	19,0	13,9	16,3
1550	1600	23,8	42,8	24,2	40,6
1500	1550	29,5	72,3	38,0	78,6
1450	1500	24,1	96,4	43,8	122,4
1400	1450	22,4	118,8	49,8	172,2
1350	1400	20,7	139,5	50,7	222,9
1300	1350	22,9	162,4	59,1	282,0
1250	1300	16,4	178,8	43,4	325,5
1200	1250	21,5	200,3	58,7	384,2
1150	1200	23,9	224,2	70,3	454,5
1100	1150	24,5	248,7	78,5	533,0
1050	1100	26,8	275,5	93,5	626,6
1000	1050	26,3	301,8	98,4	724,9
950	1000	20,3	322,1	79,9	804,8
900	950	15,8	337,9	64,2	869,0
850	900	16,2	354,1	67,8	936,8
800	850	14,7	368,8	64,4	1001,1
750	800	11,6	380,4	53,8	1055,0
700	750	8,5	388,9	41,9	1096,9
650	700	5,1	394,0	25,5	1122,4
600	650	0,9	394,9	4,6	1127,0

Appendix F: MODIS satellite images of Vatnajökull and vicinity 2011-2012.

Left: September 14th 2011; end of summer2011, obvious snowfall in NE storms. Tephra from the Grímsvötn eruption in May 2011 visible on the western and south glacier. Right: October 7th, winter conditions, September to mid-October with high winds and precipitation.

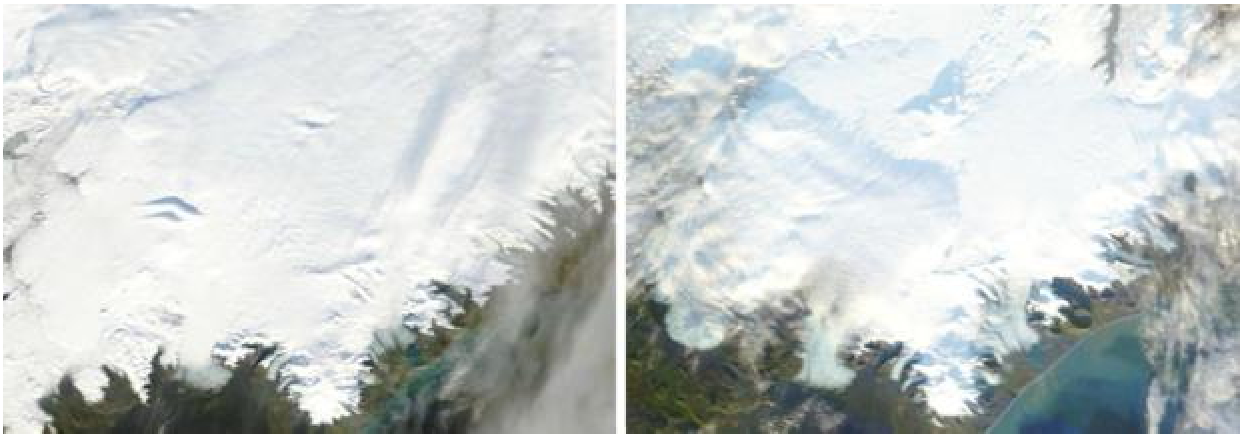

Left: October 24rd. Snow covers all Vatnajökull down to an elevation of ~400 m in the south. In the autumn field trip this week we measured up to 1.8 m thick fresh snow in the upper areas. Right: November 19th.

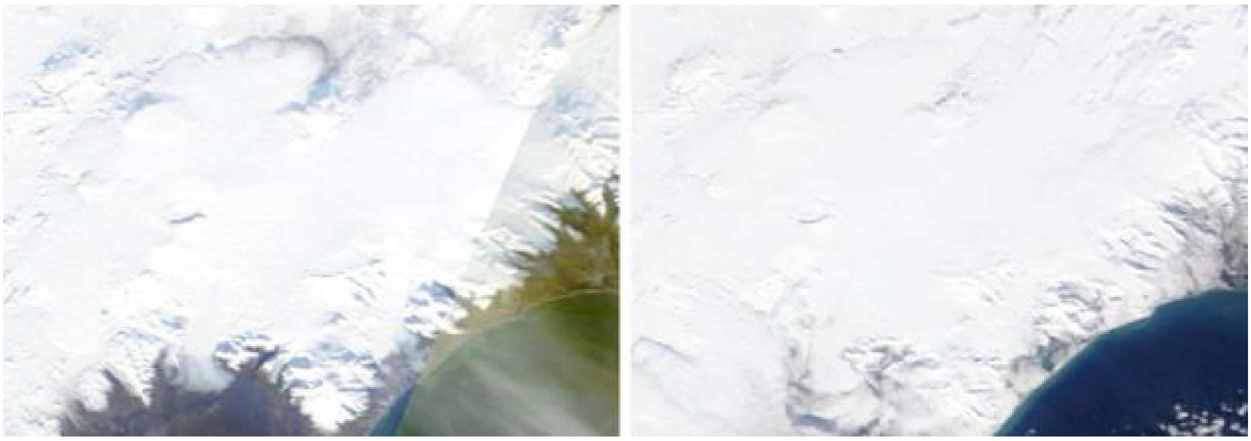

Left: February 5th, 2012. Note that the snow cover north of Vatnajökull is very thin; colours of the ground are visible. Right: April 2nd, snow cover even at close to sea level.

Left: May 3rd, most of the snow north of Vatnajökull has already melted, the winter snow cover there was thin.
Right: May 28th, dirt from the dry frontal areas has been blown over the glacier, even some areas over 1600 m in elevation are dirty. The thin snow cover on the glacier snouts has disappeared (melted).

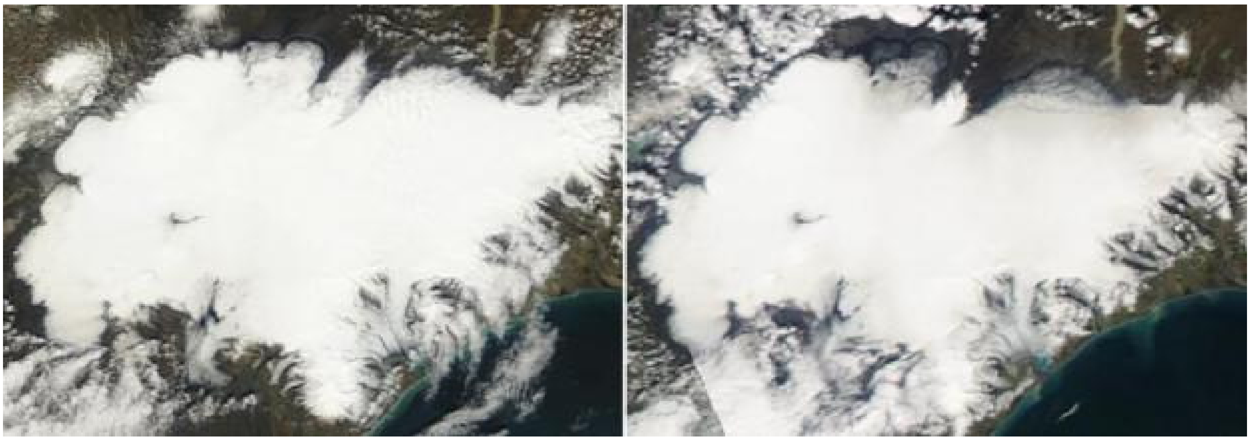

Left: June 9th, snowfall has cover most of surface dirt visible in late May, ablation almost stopped for a while in a cold spell.
Right:June 22nd, increased ablation, some of the dirty surface areas are visible again. The snow line has moved significantly upwards on the northern outlets where the snow cover was thin and dirty.

Left: July 12th, most of the surface dirty, snowline still migrating upwards.   Right: July 28th, snowline still migrating upwards on all outlets.

Left: August 26th. There has been significant ablation at the western and south outlets, but fresh snow has covered the upper areas and NE outlets. Right: September 2nd (east) and 7th (west), fresh snow in upper areas.

Left: September 12th, snowfall in cold northern storms, a chain of low pressure fields with high wind and precipitation followed. Right: September 25th, snow in the upper areas is thickening.

Left: October 5th and Right October 14th. Winter has settled in, snow cover up to 1.7 m was measured in the autumn mass balance expedition (October 8-14th).

The images are either from the MODIS Aqua or MODIS Terra satellites, visible light, 250m resolution.
http://rapidfire.sci.gsfc.nasa.gov/
The Moderate Resolution Imaging Spectroradiometer (MODIS) flies onboard NASA's Aqua and Terra satellites as part of the NASA-centered international Earth Observing System. Both satellites orbit the Earth from pole to pole, seeing most of the globe every day. Onboard Terra, MODIS sees the Earth during the morning, while Aqua MODIS orbits the Earth in the afternoon.

On the next pages MODIS images for all days of May, June, July, August and September are shown.

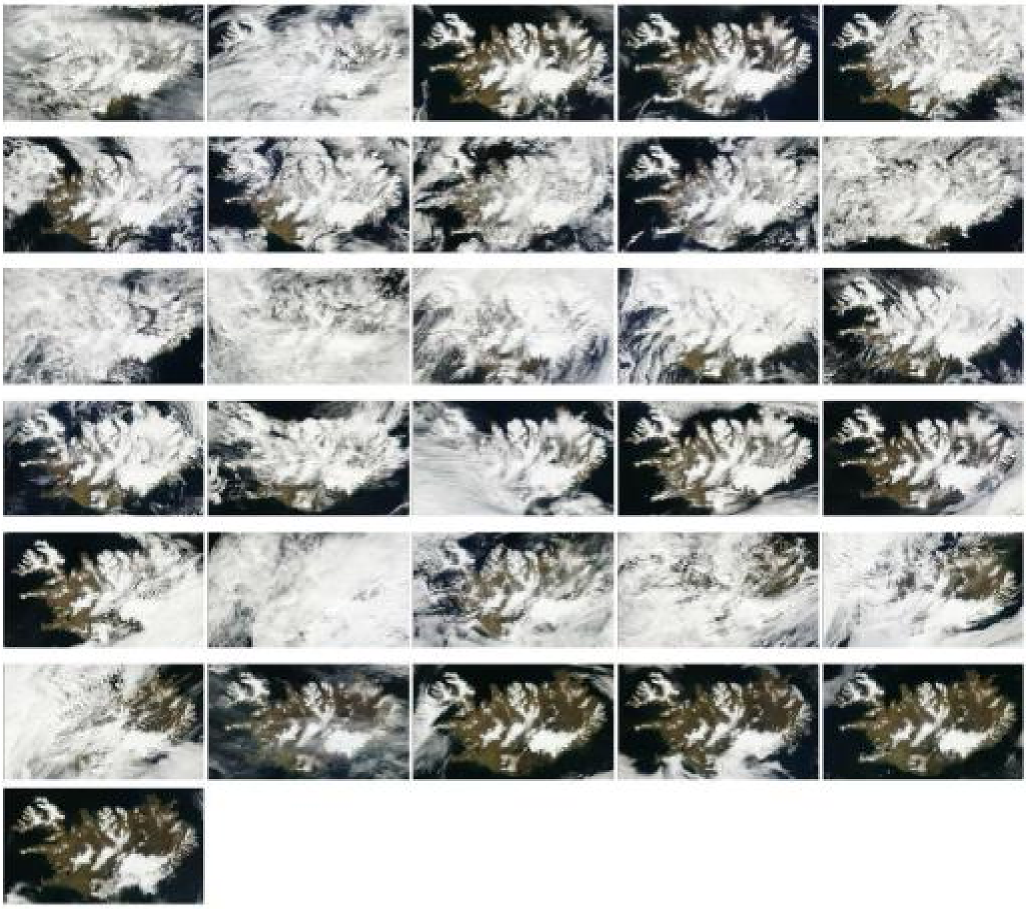

MODIS: May 2012 (read from left to right and downwards).

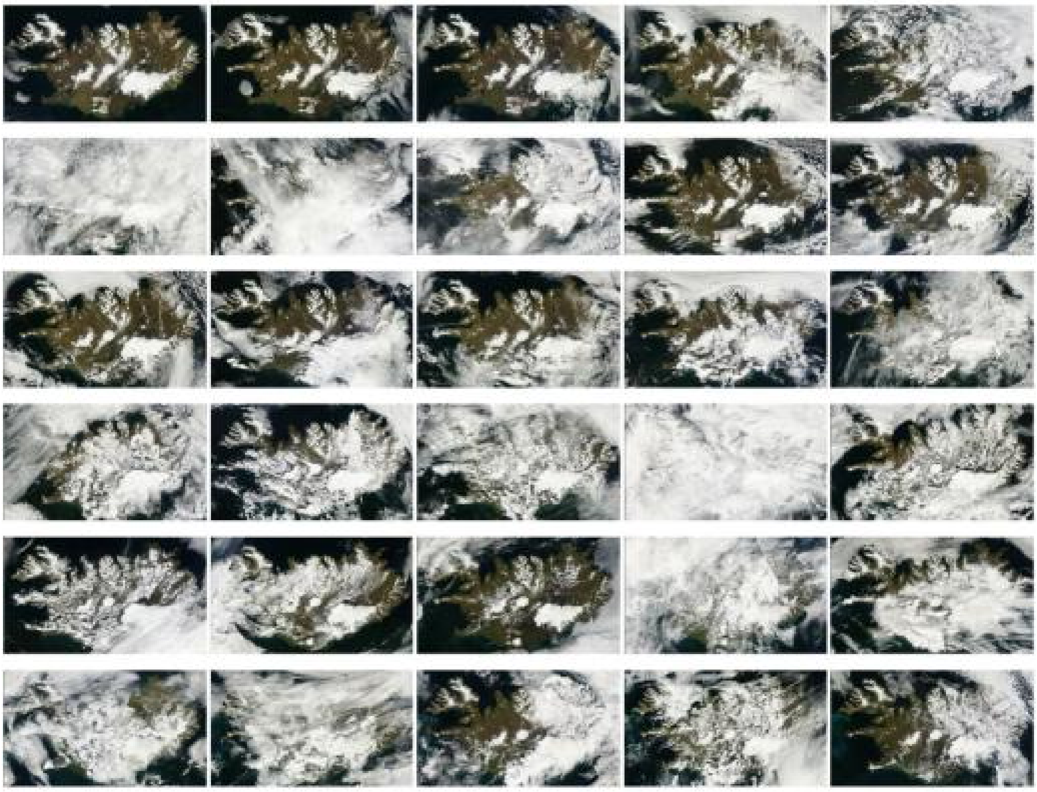

MODIS June 2012.

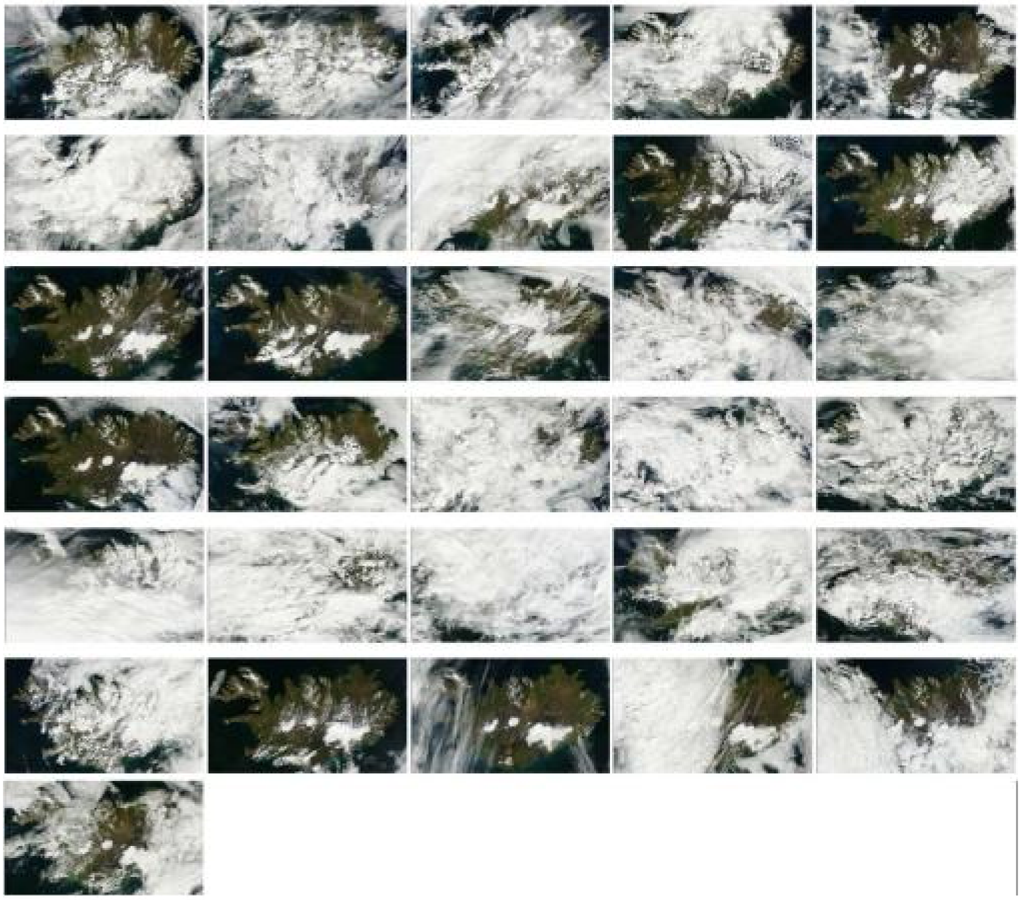

MODIS July 2012.

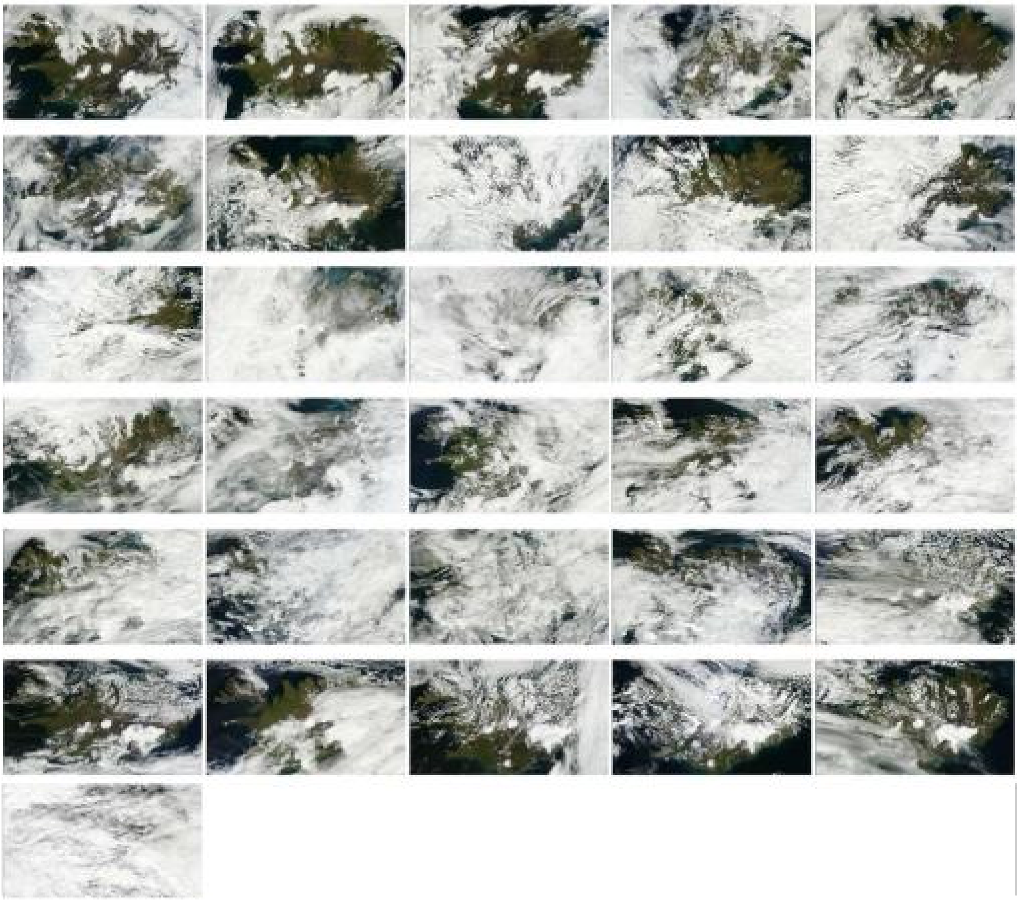

MODIS August 2012.

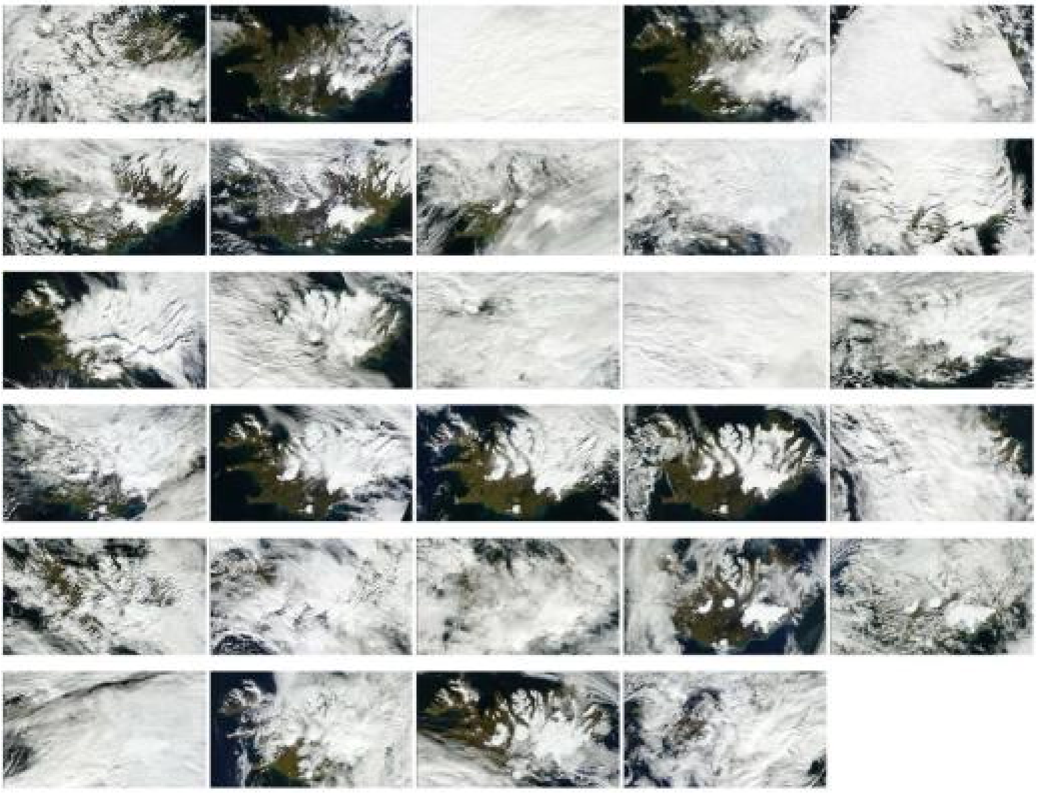

MODIS September 2012.